We are IntechOpen, the world's leading publisher of Open Access books Built by scientists, for scientists

4,800
Open access books available

122,000
International authors and editors

135M
Downloads

Our authors are among the

154
Countries delivered to

TOP 1%
most cited scientists

12.2%
Contributors from top 500 universities

CLARIVATE ANALYTICS

BOOK CITATION INDEX

INDEXED

WEB OF SCIENCE™

Selection of our books indexed in the Book Citation Index
in Web of Science™ Core Collection (BKCI)

Interested in publishing with us?
Contact book.department@intechopen.com

Numbers displayed above are based on latest data collected.
For more information visit www.intechopen.com

Computational Tools to Study and Predict the Long-Term Stability of Nanowires.

Martin E. Zoloff Michoff[1], Patricio Vélez[1],
Sergio A. Dassie[2] and Ezequiel P. M. Leiva[1]
INFIQC,
[1]Departamento de Matemática y Física
[2]Departamento de Fisicoquímica,
Facultad de Ciencias Químicas, Universidad Nacional de Córdoba
Argentina

1. Introduction

"The era in which the number of transistors on a computer chip doubles at a constant rate is drawing to a close". This is not the prophecy of an obscure mind, but is more or less the conclusion drawn by none other than the man who coined Moores´ law[1]. In an interview held in 2007, Gordon Moore recognized that by about 2020, his law would come up against the laws of physics. Furthermore, he recognized a change in a paradigm: the replacement of the top-down approach currently used for building circuits by a bottom-up procedure, where chips would be assembled using individual atoms or molecules. This is nothing but the realm of nanotechnology, while there is some consensus that the elementary switches of these circuits should be molecules with some feature allowing for the on/off status required for the components of logical devices, many questions remain concerning their stability. In the case of micrometric circuit components temperature may be an issue, but in the case of single molecules thermal effects may be overwhelming, since current flow occurs across a single bond. The lifetime of this bond, will determine the lifetime of the circuit component. Under these conditions, circuit engineering will be coming unexpectedly close to chemical kinetics.

It still is far from clear which will be the technological procedure for the massive production of these molecular circuits. However, there are a number of experimental techniques for the study of their properties that are well established. These are shown schematically in Fig. 1. Fig. 1d shows a method devised to study the structure of monatomic nanowires (NWs). It has been developed by Kondo and Takayanagi (Kondo & Takayanagi, 1997) using *High Resolution Transmission Electronic Microscopy* (HRTEM) and allows the generation of suspended NWs. In this approach nanowires are generated *in situ* by focusing an electron beam on adjacent sites of a self-supported metal thin film (*ca.* 3 nm), making holes and allowing them to grow until a nanometric bridge is formed inside or between grains. The

---

[1] Times Online September 19, 2007,
http://technology.timesonline.co.uk/tol/news/tech_and_web/article2489053.ece

relatively long lifetimes of these metallic nanowires (of the order of seconds and even minutes) allows for a detailed characterization of their geometries. This method has even been used to study the structure of alloyed metal monatomic nanowires (Bettini et al., 2006). However, because of the preparation procedure, these nanowires are susceptible to contamination by light impurity atoms (Galvão et al., 2004; Legoas et al., 2002; Legoas et al., 2004), not observed directly in the HRTEM, that affect their structure upon insertion in the monatomic chain.
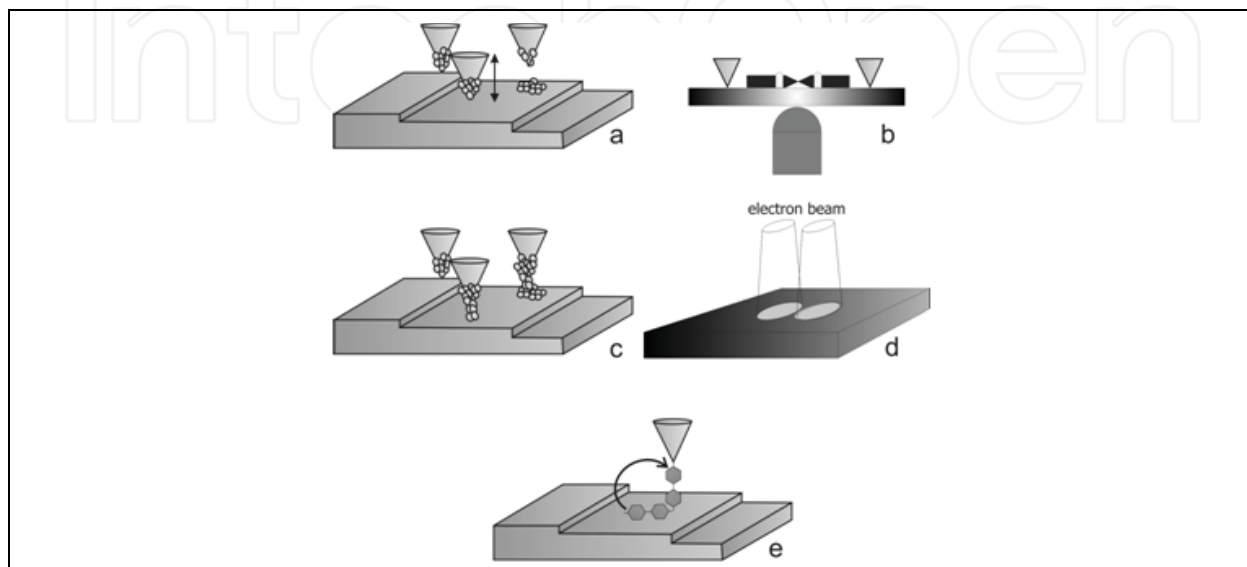

Fig. 1. Different methods employed to generate suspended nanowires: a) metallic jump-to-contact, b) mechanically controllable break-junction, c) electrochemical growth, d) electron beam punching, and e) molecular jump-to-contact.

Another procedure that has been used to study the properties of monatomic metal contacts is the so-called *Mechanically Controllable Break-Junctions* method (MCBJ, Fig. 1 b). In this technique, a metal wire is mechanically broken by mounting its two ends on a bendable substrate. In this way, the length of the contact can be adjusted by controlling the bending of the substrate. Lithographic designed MCBJ provides highly stable electrodes, with standard deviations of less than 1 pm over 24 h at low temperatures. A detailed discussion on this technique has been given by van Ruitenbeek et al. (van Ruitenbeek et al., 2005). The metal neck at the MCBJ can be also tuned by electrochemical methods as long as the metal involved can be deposited electrochemically. The main drawbacks of this technique are the lack of information on the atomic configuration, and the fact that both electrodes must be made of the same metal. The former situation was challenged recently by Yoshida et al. (Yoshida et al., 2007), who developed MCBJ inside a HRTEM chamber that allows for simultaneous performance of conductance measurements and electronic imaging of the atomic chain.

In the case of metallic *Scanning Tunnelling Microscopy* (STM) and conducting *Atomic Force Microscopy* (AFM) break junctions (Ohnishi et al., 1998; Rubio-Bollinger et al., 2001; Xu et al., 2003a; Xu & Tao, 2003), the sharp tip of the scanning probe microscope is approached to the surface and brought into contact with it (Fig. 1a). The surface may be made either of the same material as the tip or of a different one containing islands of the tip material. Upon retraction, an atomic chain of atoms occurs, whose properties are analyzed. When employed in an *Ultra High Vacuum* (UHV). The main drawbacks of this technique are the need for an

intensive cleaning procedure and the implementation of thermal and mechanical stability conditions, as it is the case of STM. On the other hand, this methodology can be used *in situ* for electrochemical experiments. In fact, it has been employed by Tao and co-workers to perform conductance measurements with Au nanowires under a variety of experimental electrochemical conditions (He et al., 2002; Xu et al., 2003b), including the properties of the nanojunction when molecules are inserted into it (Xu et al., 2003a; Xu & Tao, 2003). Efficient electrochemical methods for the generation of nanowires have also been developed. Li and Tao (Li & Tao, 1998) managed to bridge the gap between an STM tip and a substrate by a suitable potential control of both the tip and the surface(Fig. 1c). In a similar procedure, the gap between two supported metal pieces was filled by a nanometric wire using an adequate feedback electronic setup (Li et al 1999). The latter procedure has the advantage of removing thermal drift problems.

Finally, the method developed Haiss et al. moves more into the spirit of bottom up nanostructuring (Fig. 1e). In this procedure, a molecule bridges spontaneously the gap between an STM tip and a surface (Haiss et al., 2004; Haiss et al., 2006). The substrate-tip connection is verified by jumps in the tunnelling current measured.

2. Structure and stability of pure and contaminated metallic monatomic nanowires

2.1 Experimental measurements

The conductance measured through metallic monatomic nanowires is quantized in units of $G_0 = 2e^2/h$ (where e is the charge of an electron and h stands for Planck's constant). The force during the fabrication and breaking of a gold nanowire was measured using a specific STM supplemented with a force sensor at room temperature (Rubio-Bollinger et al., 2001). Force and conductace curves were thus obtained simultaneously. The later displayed a steplike behavior down to a value close to one conductance quantum (G_0), which corresponds to a one-atom contact, while the force curve showed a sawtooth like signal decreasing in amplitude in a sequence of elastic stages separated by sudden force relaxations. In this experiments the one-atom contact of gold was further stretched a distance of about 1 nm while the conductance remained close to G_0, which signals the formation of a chain of about four atoms long that finally breaks. This corresponds to a monatomic neck of ~4 gold atoms. Similar observations were made in STM experiments at 4 K (Yanson et al., 1998), and from direct observations by means of HRTEM measurements (Ohnishi et al., 1998; Rodrigues & Ugarte, 2001a; Rodrigues & Ugarte, 2002; Rodrigues et al., 2000).

Due to the inherent irreproducibility of the contacts formed, and therefore of the measured conductance curves, it is useful to construct histograms with a few hundred measured curves. A force histogram for the Au nanowire showed a narrow distribution centered at 1.5 ± 0.3 nN for the force needed to break one single bond in the chain (Rubio-Bollinger et al., 2001).

Although gold has been the most prominent metal studied so far, mechanical elongation has shown to be useful to fabricate nanowires of Ag (Rodrigues et al., 2002), Co, Pt (Rodrigues et al., 2003), Pd (Kiguchi & Murakoshi, 2006; Rodrigues et al., 2003) and Cu (Bettini et al., 2006), as well as for Au and Ag alloys of varying compositions (Sato et al., 2006b).

Two striking experimental features have drawn the attention of the researches in the last few years: first, the existence of unusually large Au – Au distances in the order of 3.6 – 4.0 Å (Kizuka, 2008; Koizumi et al., 2001; Ohnishi et al., 1998; Sato et al., 2006b), longer than the bulk distance of 2.88 Å. These experimental observations along with the simulation of

HRTEM measurements suggest that the atomic-sized wires are complexed with light elements (such as H, C, S for example) (Kizuka, 2008; Koizumi et al., 2001).

Second, the long-term stability of gold nanowires at room temperature, in many cases in the order of seconds (Legoas et al., 2002; Ohnishi et al., 1998; Rodrigues & Ugarte, 2001a; Rubio-Bollinger et al., 2001; Takai et al., 2001; Yanson et al., 1998), which is an extremely long time in relation to those characteristic of molecular motion. For instance, Fig. 2 shows the time evolution of gold chain under elongation, which is in the order of ~1 second.
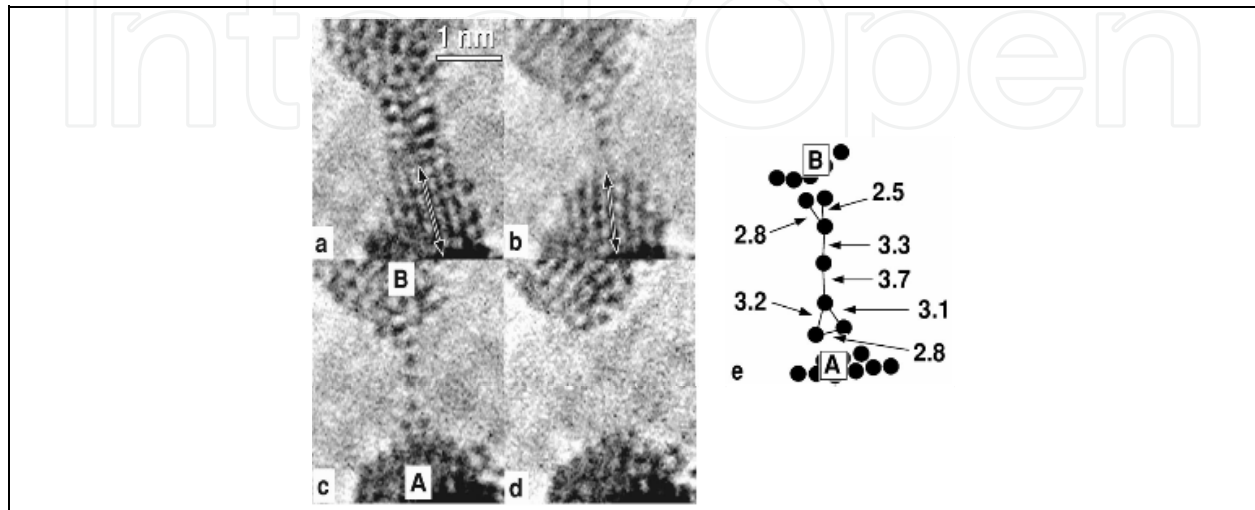

Fig. 2. Time sequence of atomic resolution images of the formation, elongation and fracture of a suspended chain of gold atoms: (a) 0 s; (b) 0.64 s; (c) 1.12 s; and (d) 3.72 s. Atomic positions appear as dark lines or dots. A schematic representation of the chain structure is shown in (e) (distances are marked in Å and the error bar is 0.1 Å); the letters A and B indicate the apex position in (c). Note that the chain is attached to the tips through a two atom structure. The double arrows in (a) and (b) have been drawn to indicate the movement (rotation) of the lower apex. Reprinted figure with permission from Rodrigues, V.; Ugarte, D. *Phys. Rev. B*, Vol. 63, No.7, 073405 (pp 1-4), 2001. Copyright 2001 by the American Physical Society.

The stability and breakdown of gold nanojunctions at different stretching rates has recently been measured by Huang et al. (Huang et al., 2007a). Information about the lifetime of the Au – Au bond is extracted from the length of the last plateau in the conductance traces of Au – Au point contacts. The most probable stretching distance for this last plateau (corresponding to an atom-sized contact between the electrodes as verified by its conductance at a G_0 value) maintains a constant value of ~0.1 nm at low stretching rates (0.8 – 8.3 nm/s). At high stretching rates (45.9 – 344 nm/s) a maximum plateau of ~0.17 nm is reached. Between these two plateaus, a linearly proportional regime is observed between the most probable distance and the logarithm of the stretching rate. This three-phase regime (illustrated in Fig. 3) has also been observed in the breakdown of biological molecules measured by AFM (Auletta et al., 2004; Merkel et al., 1999; Schönherr et al., 2000; Zou et al., 2005). The linear increase in stretching distance is related to the stretching rate according to Eq. 1 (Evans & Ritchie, 1997; Evans, 1999; Evans, 2001).

$$L^* = \frac{k_B T}{k_s x_\beta} \ln\left(\frac{t_{off} k_s x_\beta}{k_B T} \right) + \frac{k_B T}{k_s x_\beta} \ln \upsilon \qquad (1)$$
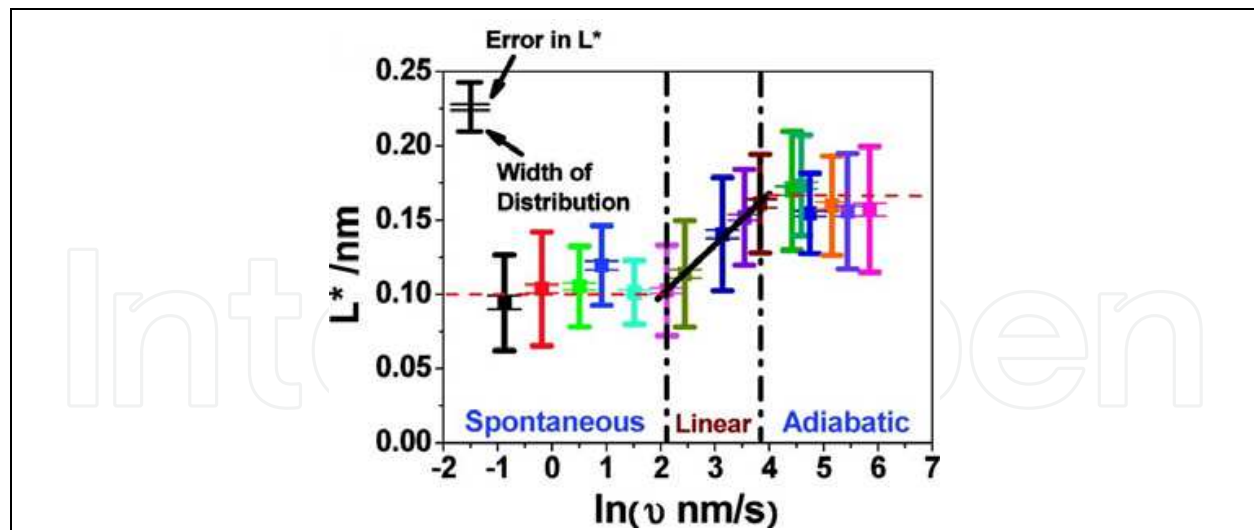
Fig. 3. Most probable stretching distance, L^*, vs logarithm of stretching rate for a Au – Au point contact. The black line is the linear fit of L^* with the logarithm of the stretching rate, according to Eq 1. Reprinted with permission from Huang, Z. F.; Chen, F.; Bennett, P. A.; Tao, N. J. *J. Am. Chem. Soc.*, Vol. 129, No.43, 13225-13231, 2007. Copyright 2007 American Chemical Society.

In Eq. 1 L^* is the most probable stretching distance, k_s is the effective spring constant of the bond, x_β is the average thermal bond length along the pulling direction until dissociation, t_{off} is the natural lifetime, and v is the stretching rate. By fitting the linear regime observed for the Au – Au point contacts to the above equation, a value of t_{off} = 81 ms was obtained.

2.2 Computational simulations

Experimental observations such as those described above, have triggered numerous theoretical approaches to gain further insight into the structure and transmission properties of these metallic nanowires. The mechanical structure and evolution of a tip-surface contact has been modelled by means of different computational techniques. In early works, *Molecular Dynamics* (MD) and effective medium theory potentials have been used to simulate the mechanical deformation of atomic-sized metallic contacts under tensile strain for Au, Ag, Pt, Ni (Bahn & Jacobsen, 2001; Dreher et al., 2005; Rubio-Bollinger et al., 2001; Sørensen et al., 1998). The relative utility of different semiempirical potentials for MD simulations of stretched gold nanowires has been recently reviewed (Pu et al., 2007a). In this work the authors find that the second-moment approximation of the tight-binding potential reproduces well the energetics of finite Au clusters. Also, the calculated tensile force just before the nanowire breaks is around 1.5 nN, consistent with the experimental result The stretching of gold nanowires has also been simulated in the presence of solvent (Pu et al., 2007b).

Tight binding MD simulations using the Naval Research Laboratory potentials, along with *ab-initio* quantum calculations within the *Density Functional Theory* (DFT) framework, provided evidence that a one-atom thick 5-atom long necklace is formed for gold nanowires under a stretching force (da Silva et al., 2001; da Silva et al., 2004). Before breaking, relatively long Au – Au distances, of the order of 3.0 – 3.1 Å are obtained, in agreement with experiments.

The main drawback of the MD simulations mentioned above is that the stretching rate used (typically in the order of 1 -2 m/s) is around 9 - 10 orders of magnitude larger than the experimental values (in the order of a tenths to a few nm/s).

The use of *ab-initio* quantum methods to study the stability of monatomic metallic nanowires is usually performed using two different methodologies. One of these procedures involves stretching the nanowire in steps of a certain elongation, minimizing the energy of the system at each step, until the breakage of the nanowire is achieved (Bahn et al., 2002; da Silva et al., 2004; De Maria & Springborg, 2000; Häkkinen et al., 2000; Nakamura et al., 1999; Nakamura et al., 2001; Novaes et al., 2003; Okamoto & Takayanagi, 1999; Rubio-Bollinger et al., 2001; Sánchez-Portal et al., 1999; Skorodumova & Simak, 2003). This method has been successfully used to, for example, predict the pulling force necessary for breaking the nanowire (da Silva et al., 2004; Nakamura et al., 1999; Novaes et al., 2003; Rubio-Bollinger et al., 2001). An alternative procedure, and more costly from a computational point of view, consists in performing *Ab-initio Molecular Dynamics* (AIMD), which has been employed to obtain a detailed description of the elongation process of pure gold nanowires (Hobi et al., 2008; Torres et al., 1999), and gold NWs in the presence of organic molecules (Krüger et al., 2002), or light weight elements as contaminants (Hobi et al., 2008; Legoas et al., 2004). AIMD takes into account the thermal motion of the system, for which in a first approach seems a more appropriate approximation to obtain reliable information about the mechanical proprieties and the stability of metallic atom-sized wires. Nonetheless, the experimental elongation times are far larger than those accessible by an AIMD simulation, typically in the order of nanoseconds.

As it was mentioned above, one of the possible explanations for the rather long Au – Au distances observed in a monatomic neck is the presence of light weight elements, such as C, H, O or S, intercalated between gold atoms. This possibility has only been investigated so far by the means of computational simulations, since these light weight elements would have a low contrast against the much heavier Au atoms, and thus rendering their direct visualization by today's electronic microscopes very difficult. Carbon is a frequent contaminant in bulk gold (Legoas et al., 2002), while hydrogen (O'Hanlon, 2001) and oxygen (Bahn et al., 2002) are impurities very difficult to extract even in the best UHV conditions. Although the possibility of hydrogen acting as a contaminant has been ruled out by an AIMD study (Legoas et al., 2004), this result has been subsequently challenged (Hobi et al., 2005).

Legoas et al. (Legoas et al., 2002) modelled monatomic gold chains contaminated with carbon by means of geometry optimization at DFT-LDA level. The authors used an isolated linear chain and no tension was exerted on the system. Their results showed that long Au – Au distances of around 4 – 4.5 Å could be explained by the presence of two consecutive carbon atoms (C_2) inserted into the gold chain. Whereas, another set of anomalously long bond in the order of 3 – 3.7 Å could be a consequence of a mixture of pure Au – Au bonds with contamination of such a bond by a single carbon atom.

Skorodumova and Simak (Skorodumova & Simak, 2003) showed, using DFT-GGA calculations, that the unusual structural stability of monatomic gold wires could be explained in terms of hydrogen contamination. Stretching the nanowire, the authors observed that the chain takes a linear structure with hydrogen atoms intercalated and a Au – Au distance of 8.8 Å before the nanowire breaks. The cohesive energy of the contaminated gold wire was found to be 2-fold higher than a pure chain of gold atoms. This last result was attributed to a partial charge transfer from gold to hydrogen. Subsequently, the influence of

carbon was explored using the same computational methodology (Skorodumova et al., 2007; Skorodumova & Simak, 2004), also finding that carbon can enhance the stability of linear gold chains yielding large interatomic distances.

Novaes et al. (Novaes et al., 2003) studied through *ab- initio* calculations the effect of H, B, C, N, O and S impurities on a gold nanowire electronic and structural properties. The authors find that the most likely candidates to explain the distances in the range of 3.6 Å and 4.8 Å are H and S impurity atoms, respectively.

The main drawback of the procedures presented so far is that the presence of the impurity is simply assumed, and no description is obtained of how, when, or with what probability it migrates to the position it was assumed to have. To overcome this limitation, an AIMD study of the formation and growth of gold chains with a variety of impurities (H, C, O, S), without any assumption of their initial positions was performed (Anglada et al., 2007). One or two impurity atoms were introduced randomly in an amorphous column of 50 – 150 gold atoms. These amorphous solid columns were stretched during 4 – 18 ns until they broke. Hydrogen was always found to evaporate before formation of the monatomic chain took place. Carbon and oxygen were found in the final chains with low probability (~ 10 %), while sulphur was found participating in it with a high probability (~ 90 %). The mean distances between gold atoms bridged by C, O and S were 3.3, 3.4 and 5.0 Å, respectively, in good agreement with experiments.

Inasmuch as this last study provides a level of accuracy and reliability superior to those mentioned before, the stretching rate is still much higher than those typically used in experiments, and the simulations last only a few nanoseconds, while experiments take place in the order of 0.001 – 1 second.

The study of the effect of impurities on the structure and stability of gold nanowires is an ongoing investigation topic. Some of the most recent theoretical work can be found in (Jelínek et al., 2008; Novaes et al., 2006; Zhang et al., 2008). Although gold is by far the most prominent element of interest in the formation of nanowires, some recent computational studies have also involved copper nanowires (Amorim et al., 2007; Amorim et al., 2008; Sato et al., 2006a).

3. Single molecule nanowires

3.1 Experimental measurements

Building a device in which a single molecule bridges two metallic electrodes is of major interest, since one could easily tailor the nanojunction electronic properties by changing the molecule or even only a substituent in the molecule. This opens an enormous range of possibilities in the field of molecular electronics.

Most of the experimental (Cui et al., 2001; Haiss et al., 2004; Haiss et al., 2006; Huang et al., 2006; Huang et al., 2007a; Huang et al., 2007b; Li et al., 2007a; Li et al., 2006a; Xu et al., 2003a; Xu et al., 2005; Xu & Tao, 2003) and computational work (Batista et al., 2007; Hou et al., 2005; Hou et al., 2006; Kim et al., 2006b; Li et al., 2005; Li et al., 2006b; Li et al., 2006c; Paulsson et al., 2008; Perez-Jimenez, 2005; Stadler et al., 2005; Wu et al., 2005) performed with this systems deal with the measurement and/or theoretical determination of the conductance of the molecular nanojunction, particularly those in which the linker atom to the metallic electrodes is either S or N. For a recent review on some of these aspects readers can refer to (Vélez et al., 2007).

The chemical identity of the linker moiety plays a fundamental role in determining both the electrical and mechanical properties of the molecular nanojunction. Without discussion the most widely used anchoring group is thiol (Chen et al., 2006; Haiss et al., 2008; Haiss et al., 2009; Huang et al., 2006; Huang et al., 2007a; Huang et al., 2007b; Li et al., 2007b; Li et al., 2006a; Ulrich et al., 2006; Xu et al., 2003a; Xu et al., 2005; Xu & Tao, 2003), although pyridine (Xu et al., 2003a; Xu & Tao, 2003), isocyanide (Beebe et al., 2002; Kiguchi et al., 2006; Kiguchi et al., 2007; Kim et al., 2006a), selenium (Patrone et al., 2003a; Patrone et al., 2003b; Yasuda et al., 2006), amine (Chen et al., 2006; Hybertsen et al., 2008; Kamenetska et al., 2009; Kiguchi et al., 2008; Park et al., 2007; Park et al., 2009; Quek et al., 2007; Quek et al., 2009; Quinn et al., 2007; Venkataraman et al., 2006a; Venkataraman et al., 2007; Venkataraman et al., 2006b), phosphines (Kamenetska et al., 2009; Park et al., 2007) and carboxylate (Chen et al., 2006; Martín et al., 2008) have proved to provide enough binding strength to yield a stable contact. In most of these works, the metallic electrodes that the molecule bridges are made of gold, but some recent reports showed the utility of platinum electrodes for those purposes (Kiguchi et al., 2007; Kiguchi et al., 2008).

Xu et. al. reported the first electromechanical measurement of a molecular junction (Xu et al., 2003a). The authors determined simultaneously the conductance and the force under mechanical stretching for the octanodithiol (ODT) and 4,4'-bipyridine (BYP) nanojunctions. The quantum conductance for BYP resulted 40 times larger than that of ODT, while the force quantum was 0.8 ± 0.2 nN, considerably smaller than the 1.5 ± 0.2 nN determined for ODT. This last value is the same as that required to break a Au – Au bond (Rubio-Bollinger et al., 2001). Thus, the authors concluded that the breakdown of the ODT nanojunction involves a Au – Au bond rupture, whereas in the case of BYP, the lower breaking force would indicate that a Au – N bond is breaking. These results are in agreement with the notion of the Au- S bond being stronger than the Au-N bond (Stolberg et al., 1990). In a subsequent study, Huang et. al. found that the behavior of the ODT nanojunction as a function of the stretching rate is essentially identical to that of a pure gold point contacts (Huang et al., 2007a).

One useful experimental parameter to determine how strong is the molecule bonded to the metallic electrodes is the length that the junction formed by a single molecule can be stretched before it breaks. This allowed Kiguchi et. al. to establish the following order in binding energies for 1,4-disubstituted benzenes with Au and Pt electrodes: $Au\text{-}NH_2$ < Pt-NH_2 ~ Au-S < Au-isoCN < Pt-isoCN ~ Pt-S (Kiguchi et al., 2006; Kiguchi et al., 2007; Kiguchi et al., 2008).

The statistical analysis of the stretching length was also used to establish the following order in the sense of increasing binding strength: Au-COOH < $Au\text{-}NH_2$ < Au-S (Chen et al., 2006).

3.2 Computational simulations

As mentioned above, a large proportion of the theoretical work on molecular nanowires involves the calculation of the conductance. Only a few of these have addressed some aspects of the thermodynamic stability of such nanocontacts.

As it respects to the mechanical properties of a molecular nanojunction, one or the first *ab-initio* studies was performed by Krüger et. al. (Krüger et al., 2003). A thiomethyl radical bonded to a 5-atom planar cluster was used as a model for a typical Au – S contact. The junction was elongated, with geometry optimization at each step, obtaining an isomerization of the cluster into a linear chain which finally breaks at a Au – Au bond with a force of ~ 1.5 nN. In a Car-Parrinello molecular dynamics the same authors showed that when ethylthiol attached to a gold surface is pulled, this leads to the formation of a monoatomic gold

nanowire, followed by breaking a Au – Au bond with a rupture force of about 1.2 nN (Krüger et al., 2002).

In a different study, the stretching and breaking behavior of a benzene dithiol molecule sandwiched between two Au(111) slabs was studied using DFT calculations (Lorenz et al., 2006). It was found that breakage occurs through a dissociation of one of the Au – S bonds with a maximum force of 1.25 nN in the case when the molecule is directly attached to the surface, and of 1.9 nN when an adatom is placed between the sulphur and the gold slab.

Similar studies were carried out for nanojunctions involving 4,4'-bipyridine (Stadler et al., 2005; Vélez et al., 2005), pyrazines (Vélez et al., 2005; Zoloff Michoff et al., 2009), amines (Hybertsen et al., 2008; Kamenetska et al., 2009), and alkylphosphines (Kamenetska et al., 2009). Binding energies and rupture forces are the parameters that can be obtained from these types of computational simulations that can be related to the mechanical stability of the molecular nanojunction. It should be noticed that temperature activated processes are not considered in these calculations.

4. Long term stability of metallic monatomic nanowires

As can be gathered from the summary of the computational work performed so far with the aim of obtaining valuable information about the stability of NWs, the main challenge remains to develop models that would allow to use this valuable computational information to extrapolate to the experimental time scale, and taking thermal motion into account. In the following sections a simple kinetic model based on the *Transition State Theory* (TST) is presented. The utility of this model along with DFT calculations and an exploration of the energy landscape with a suitable algorithm will be illustrated for pure and contaminated gold monatomic NWs, as well as for single molecule contacts.

4.1 The minimum energy path and the transition state theory

A common and important problem in theoretical chemistry and solid state physics is to identify the path with the lowest energy for the reorganization of a group of atoms from a stable configuration to another. This path is referred to as the *Minimum Energy Path* (MEP) and is often used to define a *Reaction Coordinate* (RC) for transitions of the type of chemical reactions, conformational changes in molecules or diffusion processes in solids. The maximum potential energy along the MEP is referred to as the *saddle point*, and provides the activation energy for the occurrence of the process. To calculate the transition rate constant is of central importance in the TST (Eyring, 1935; Vineyard, 1957), as will be discussed in section 4.2.

Different methods have been developed to find the reaction path and saddle points (Michael & Michael, 2007). We focus our attention on methods that make use of two boundary conditions: the initial and final configurations for the transition. These settings should normally correspond to two local minima in the multidimensional potential energy surface. These minima may be obtained from different energy minimization techniques such as the simulated annealing, conjugate gradient, etc.

These methods require only the calculation of first derivatives of the potential energy. They generate a chain of images or replicas of the system between the initial and final configurations. All the intermediate images are simultaneously optimized in some concerted way of the potential energy surface that should be as close as possible to guarantee the convergence to the MEP. The method called *Nudged Elastic Band* (NEB) (Henkelman et al.,

2000; Henkelman & Jonsson, 2000; Mills & Jónsson, 1994) works in the scheme of these methods and its implementation is particularly simple. The NEB method has been successfully applied to a variety of problems, such as studies of diffusion on metal surfaces (Villarba & Jónsson, 1994), the dissociative adsorption of molecules on a surface (Mills & Jónsson, 1994), and the formation of a contact between a STM tip and a surface (Sørensen et al., 1996).

4.2 Kinetic model

As it was shown by Krüger *et. al.* in the computational simulation studies described above (Krüger et al., 2002; Krüger et al., 2003), the creation of a Au nanowire takes place in a number of steps, involving an isomerization process. Our approach will only deal with the final stage, where the NW breaks but the model could be extended to a multi-step process. We will assume that, for a given elongation of the wire, it may exist either in a *broken* (*b*) or *unbroken* (*u*) state (see Fig. 4). The related system energies are denoted with E_b and E_u, respectively. When shifting from state *u* to *b*, the system will find an energy barrier (activation energy) that we will denote with $\Delta E\ddagger$. We will neglect the reverse process in all the treatment we give below. In principle, wire reformation could be easily introduced in the model. However, we must take into account that in order to surmount the activation energies involved, the system must gain a considerable amount of energy, which will be released in the downhill stage after crossing through the maximum. This excess energy will rapidly take the systems to other more compact configurations of the final state. To be more illustrative, immediately after the rupture the wire (state *b*) will find itself in a situation where the Au atoms are in a very low coordination, so that they will stabilize by merging to
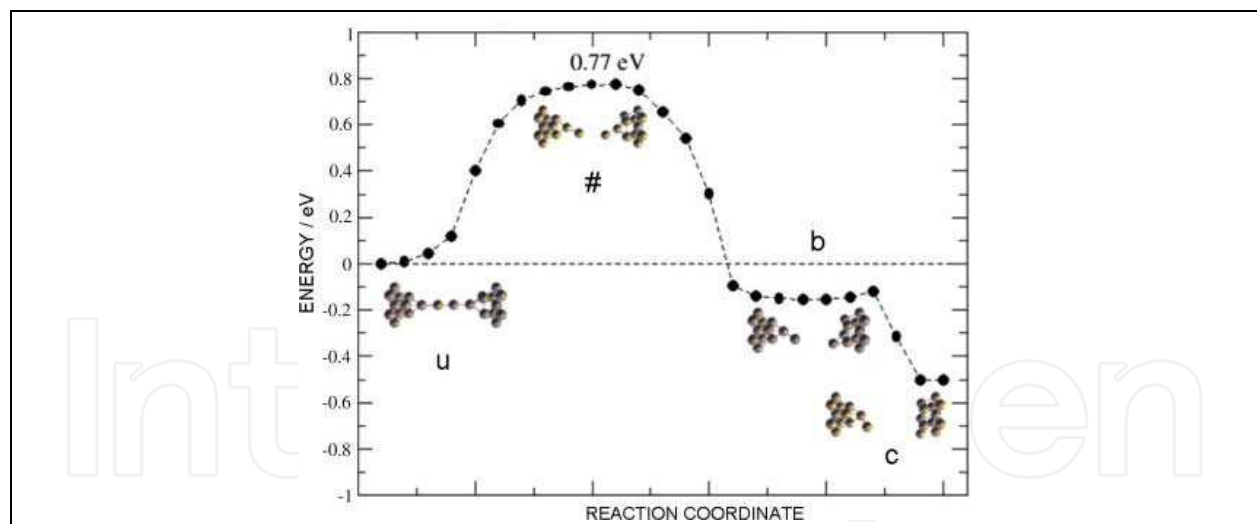

Fig. 4. Scheme of the different stages of the rupture of a Au NW. The states labelled as *u*, *b* and # correspond to the *unbroken*, *broken* and *activated* states, respectively. The state labelled as *c* indicates a situation where the broken wire has evolved towards a more compact state, in which the pieces of the broken NW are attached to the bulky pieces of the junction. Although the present figure is meant with illustrative purposes, the configurations and energies were obtained from calculations using the modified embedded atom method potentials (Baskes et al., 1989) and the nudged elastic method (Henkelman et al., 2000; Henkelman & Jonsson, 2000). Reprinted from Vélez, P.; Dassie, S. A.; Leiva, E. P. M. *Chem. Phys. Lett.*, Vol. 460, No.1-3, 261-265, 2008 with permission from Elsevier.

a bulky piece of metal of one of the tips making the junction (state *c*). These qualitative assessments are based on semiempirical calculations[2].

Following the TST, we have for the forward process (wire breaking) the frequency ν_f given by Eq. 2.

$$\nu_f = \nu_u \exp\left(-\frac{\Delta E^{\ddagger}}{k_B T} \right) \tag{2}$$

where k_B is Boltzmann's constant, T the absolute temperature, ν_u is a factor showing a weak dependence on temperature that represents an average oscillation frequency and $\Delta E^{\ddagger}$ is calculated as $E^{\#} - E_u$. Since $\Delta E^{\ddagger}$ and ν_u are in principle functions of the wire elongation, this will also be the case of ν_f. Typical values of ν_u are 3.5 – 7.0 x 10^{12} Hz (Bürki et al., 2005; Todorov et al., 2001). We have found that the assumption of constant (elongation independent) values in this range leads essentially to the same qualitative and quantitative predictions we show below. However, in order to get a parameter free description of the problem, it would be desirable to get not only $\Delta E^{\ddagger}$ but also ν_u from first-principles calculations. Sánchez-Portal et al. (Sánchez-Portal et al., 1999) have calculated the transversal and longitudinal phonon frequencies of a Au NW by means of the frozen phonon method at different wire lengths. In order to get an estimation of ν_u for our problem, we have parameterized the results of these authors for the transversal mode as a function of the wire elongation and introduced it in our equations for ν_u (Δz).

Let us now consider a differential elongation of the wire $d\Delta z$ performed in a period of time dt. The number of crossings from state *u* to state *b* over the barrier in dt will then be given by Eq. 3.

$$dn = \left[\nu_u \exp\left(-\frac{\Delta E^{\ddagger}}{k_B T} \right) \right] dt \tag{3}$$

dn being the average number of times that the system moves from the *unbroken* to the *broken* state in the time *dt*. If we want to calculate the number of possible crossings in a finite period of time we integrate between 0 and t, which is given Eq. 4.

$$\Delta n = \int_{t=0}^{t=\tau^*} \left[\nu_u \exp\left(-\frac{\Delta E^{\ddagger}}{k_B T} \right) \right] dt \tag{4}$$

We can estimate the lifetime of the wire τ^* by setting in $\Delta n = 1$ (Eq. 5).

$$\int_{t=0}^{t=\tau^*} \left[\nu_u \exp\left(-\frac{\Delta E^{\ddagger}}{k_B T} \right) \right] dt = 1 \tag{5}$$

Note that in the present formulation no assumption has been made on how the wire is elongated. We turn now to consider two different possibilities:

---

[2] P. Vélez, S. A. Dassie, E. P. M. Leiva unpublished results.

Static rupture of the nanowire: In this case, rupture of the NW is studied at a constant elongation Δz. Under these conditions, the argument of the integral in Eq. 5 becomes independent of time and the breaking time can be straightforwardly obtained by solving Eq. 6, given below.

$$\left[\nu_u \exp\left(-\frac{\Delta E^{\ddagger}}{k_B T} \right) \right] \tau^* = 1 \tag{6}$$

Rupture of the nanowire at a constant elongation rate: If we assume that the NW is stretched at a constant rate, $d\Delta z / dt = v_e$, then we have Eq. 7, where Δz_0 is the elongation at t=0, Δz^* is the breaking elongation for the NW and we have written the activation energy as $\Delta E^{\ddagger}(\Delta z)$ to emphasize the dependence of the quantity on the elongation. ν_u was also considered to be elongation dependent and calculated as pointed out above. However, the dependence of the predictions on this parameter is rather weak. Once the dependence of $\Delta E^{\ddagger}(\Delta z)$ on Δz is given, Eq. 7 can be solved numerically to get the dependence of Δz^* on the elongation rate v_e.

$$\int_{\Delta z = \Delta z_0}^{\Delta z = \Delta z^*} \left[\nu_u \left(\Delta z \right) \exp\left(-\frac{\Delta E^{\ddagger}\left(\Delta z \right)}{k_B T} \right) \right] d\Delta z = v_e \tag{7}$$

4.2 Results for pure metallic nanowires

In order to illustrate the method, we consider a system consisting of a Au nanowire made of a supercell containing 4 atoms which are periodically repeated in space (Au_4 NW). Fig. 5 shows a scheme of the unit cell employed to simulate the Au_4 NW considered here. We used 4 atoms because the elongation distances at which a NW of this size breaks are in the range between 0.11 to 0.14 nm, which is the value that Huang et al. (Huang et al., 2007a) have found experimentally (see Fig. 9a below). Although this is a rather small system, the rupture of the wire has been found to be the displacement of one of atoms perpendicular to the wire axis (Ke et al., 2007), so that the interaction of the breaking bond with the rest of the system should be minimal. Atom 1 is fixed and the length of the supercell is stretched. For a given stretching of the NW, the energy of the system can be minimized with respect to all the atomic coordinates. Let us denote with $E_{min}(\Delta z)$ the minimum energy for a given $\Delta z = L - L_0$, where L_0 is the chain length at equilibrium for each system and L is the total chain length; at some Δz, say Δz_{min}, E_{min} will present a minimum, that we denote with $E_{min}(\Delta z)$. In the following discussion, we refer all the stretching lengths to Δz_{min} and all the energies to $E_{min}(\Delta z)$.

While the unbroken state is clearly defined, some uncertainty remains concerning the broken one. With this purpose, *ab initio molecular dynamics* simulations were performed near the point where the NW breaks, finding structures which are very similar to that proposed below in the broken state of Fig. 7, which was obtained by minimizing the energy of the systems, as were the remaining configurations. It is interesting to point out that the broken configuration is the same as one of the most stable Au_4 clusters reported in (Bonacic-Koutecky et al., 2002).
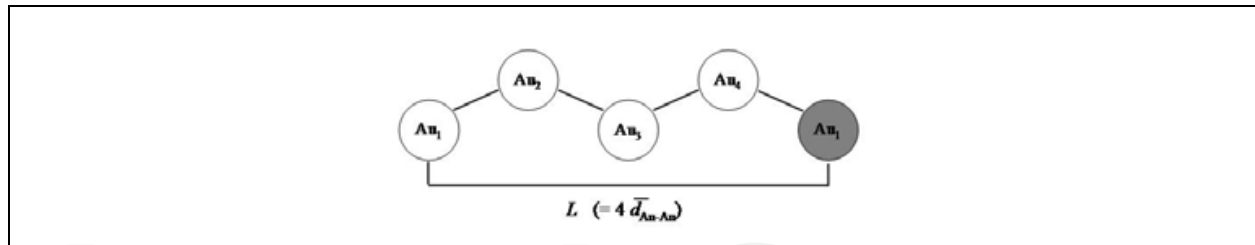
Fig. 5. Schematic representation of the unit cell employed in the present calculations. L is the total chain length and $4\overline{d}_{Au\text{-}Au}$ is the average Au-Au separation distance. Reprinted from Vélez, P.; Dassie, S. A.; Leiva, E. P. M. *Chem. Phys. Lett.*, Vol. 460, No.1-3, 261-265, 2008 with permission from Elsevier.

This configuration was then adopted to obtain the broken state for different elongations. This was achieved by compressing the system to a cell size corresponding to the desired length *L*, and then performing a conjugate gradient minimization to obtain the *broken* state for each system. The *minimum energy path* between the *unbroken* and *broken* states at each Δz, was then obtained by means of the NEB algorithm.

Curves for the energy of the *unbroken* state E_u, the *broken* state E_b, and the activated state $E^{\#}$ as a function of the wire elongation are shown in Fig. 6a. The energy curves of the *broken* and *unbroken* state meet for an elongation of $\Delta z_{u\text{-}b}$ = 0.1565 nm. At this point the activation energies for the backward and forward reactions are the same and they are equal to 0.33 eV.
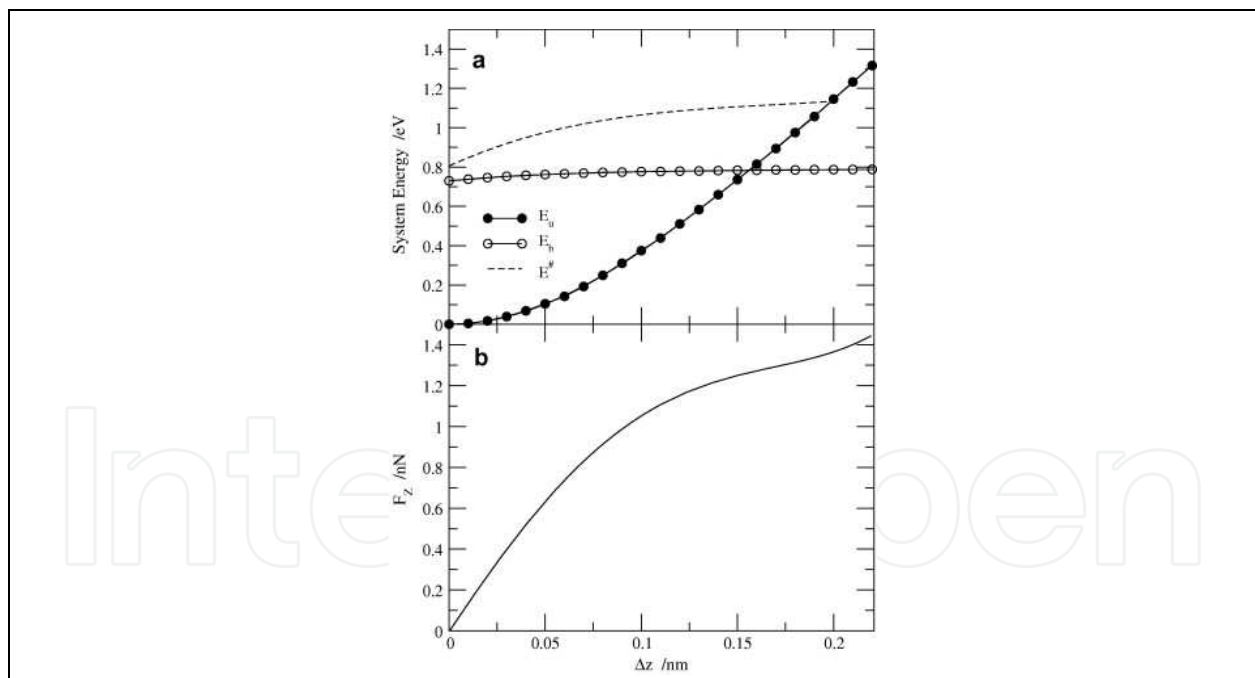

Fig. 6. System energy and force curves upon system elongation for the Au$_4$ nanowire. a) Energy of the *unbroken* state, E_u, energy of the *broken* state, E_b, and energy of the *activated* state, $E^{\#}$, as a function of the stretching of the NW, Δz. In all cases the energy of the system is referred to the minimum value that the system takes for the set of Δz considered. The activation energy for NW rupture is $\Delta E^{\ddagger} = E^{\#} - E_u$. b) Force calculated according to Eq. 8 as a function of Δz. Reprinted from Vélez, P.; Dassie, S. A.; Leiva, E. P. M. *Chem. Phys. Lett.*, Vol. 460, No.1-3, 261-265, 2008 with permission from Elsevier.

This would yield a switching frequency between the *broken* and *unbroken* state of the order of 10^6 Hz at room temperature, going down to the order of 1 Hz at 135 K. However, as we stated previously, after the bond is broken the system will immediately rearrange to other more stable configuration so that the forward reaction can be considered as irreversible under the usual stretching conditions. On the other hand, the energies of the *unbroken* and activated state meet at an elongation $\Delta z_{u-\#} = 0.1995$ nm. This represents a non-activated rupture process for the NW, and thus the Au – Au average distance at this point (*ca.* 2.88 Å) represents an absolute limit for wire stability.

Fig. 6b shows the force of the system, calculated as the component of the force applied on the NW at each step from Eq. 8.

$$F_z = -\frac{\partial}{\partial \Delta z} E_u(\Delta z) \tag{8}$$

In Fig. 7 we can observe curves for the energies of the system between *broken* and *unbroken* states at some sample elongations. From these curves it can be appreciated that the transition state is shifted towards the *broken* state. The configurations of the system at the *broken*, *unbroken*, and activated state are also shown. It is remarkable that the structure of the *broken* state is similar to the Au fragment attached to an ethylthiolate molecule, as it was found in an AIMD simulation (Krüger et al., 2002).
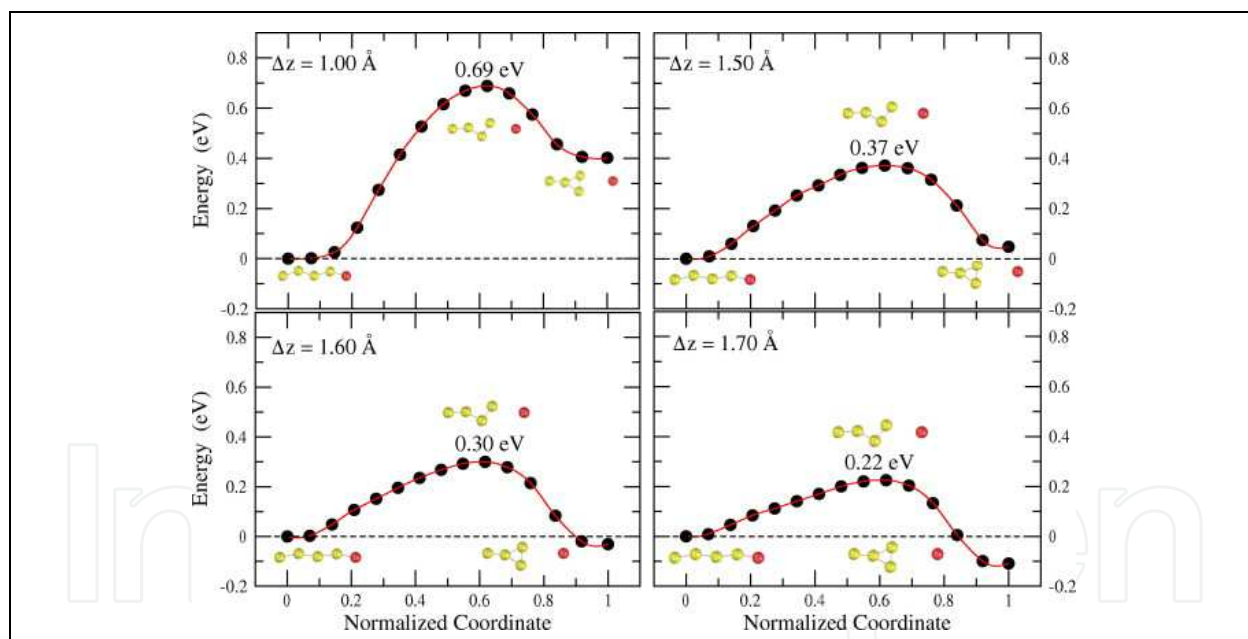

Fig. 7. Energy of the system at the reaction path between *broken* and *unbroken* states at some sample elongations. The energy is in all cases referred to the *unbroken* state. The configurations of the system at the *broken*, *unbroken*, and *activated* states are depicted within each frame. Reprinted from Vélez, P.; Dassie, S. A.; Leiva, E. P. M. *Chem. Phys. Lett.*, Vol. 460, No.1-3, 261-265, 2008 with permission from Elsevier.

Static rupture of the nanowire: A logarithmic plot for the static rupture of the NW calculated according to Eq. 6 is shown in Fig. 8. The lowest stretching rates employed in the experiments allow the rupture of NWs in times of the order of 0.1 s. Fig. 8 shows that in this order of times the wires should break at distances close to 0.105 nm. This is very close to the

experimental value of 0.1 nm (Huang et al., 2007a) obtained at the lowest stretching rates. Thus, the present results also support the general idea that long Au – Au distances such as those found in the experiments of (Legoas et al., 2002; Ohnishi et al., 1998; Rodrigues & Ugarte, 2001a; Rodrigues & Ugarte, 2001b) at room temperature cannot occur for pure Au NWs. On the other hand, at 150 K and below, pure Au NWs can be considerably stretched beyond that point.
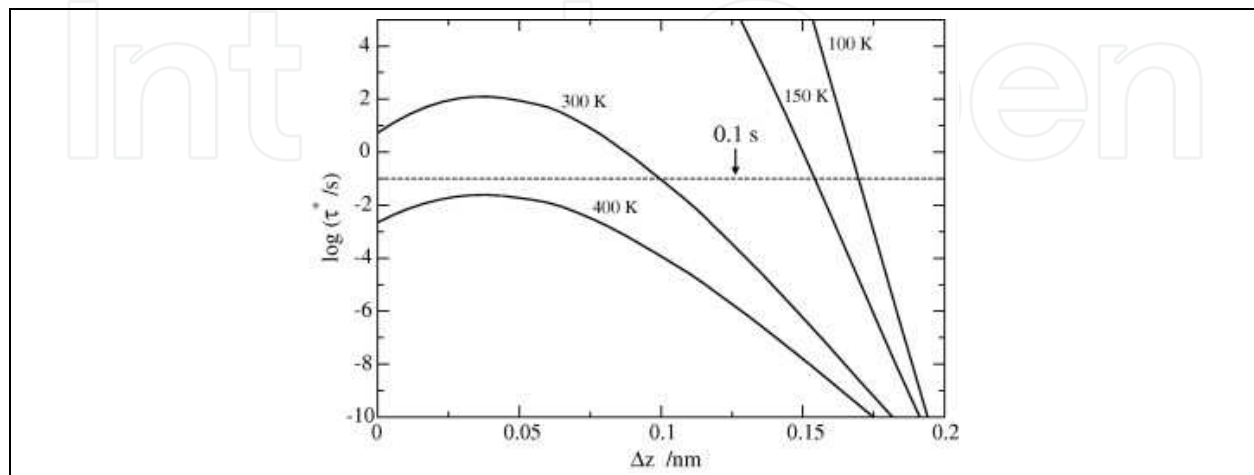

Fig. 8. Decimal logarithm of the lifetime τ^* of a Au$_4$ nanowire at different elongations calculated according to Eq. 6 for different temperatures. The dotted line denotes a constant lifetime of 0.1 s. Reprinted from Vélez, P.; Dassie, S. A.; Leiva, E. P. M. *Chem. Phys. Lett.*, Vol. 460, No.1-3, 261-265, 2008 with permission from Elsevier.
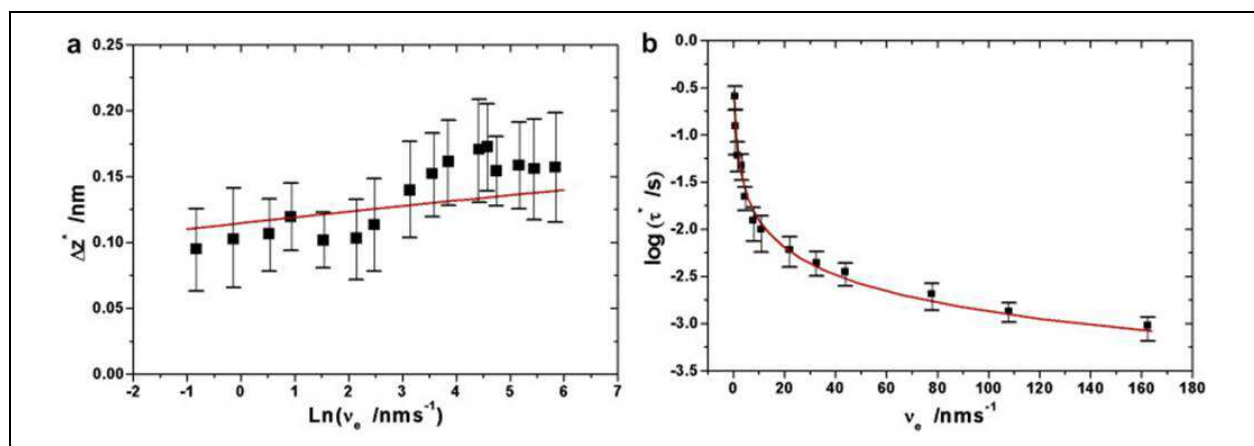

Fig. 9. Dynamic rupture of a Au$_4$ nanowire: a) Breaking distance as a function of the logarithm of the elongation rate v_e. The full line shows the calculations according to the present model and the squares are data for gold point contacts taken from (Huang et al., 2007a). The segments show the width of the distribution reported there. No fitting parameters were considered. b) Logarithm of the lifetime of the wire, τ^*, as a function of the decimal logarithm of the elongation rate, v_e. The full line shows the calculations according to the present model and the squares are experimental data for the rupture of the Au – ODT taken from (Huang et al., 2007a). The segments show the width of the distribution reported there. No fitting parameters were considered. Reprinted from Vélez, P.; Dassie, S. A.; Leiva, E. P. M. *Chem. Phys. Lett.*, Vol. 460, No.1-3, 261-265, 2008 with permission from Elsevier.

Rupture of the nanowire at a constant elongation rate: The dynamic rupture of a Au_4 nanowire was studied according to Eq. 7. Fig. 9a shows the breaking distance as a function of ln (ν_e) for elongation rates between e^{-1} and e^6 in comparison with the experimental date taken from Huang et al. (Huang et al., 2007a). It can be observed that the calculated results resemble the experimental trend in the general features.

A further point that can be analyzed through the present calculations is the lifetime of the wires as a function of the elongation rates. These results are given in Fig. 9b. There is no experimental data available for a straightforward comparison with our calculations. However, AIMD simulations (Krüger et al., 2002), and considerations based on experiments (Huang et al., 2006; Huang et al., 2007a; Li et al., 2006a) indicate that the rupture of a nanocontact made of an alkanethiol and Au contacts should break at a Au – Au bond, so that comparison between the present results may be made with the experiment of Huang et al. (Huang et al., 2007a), who have studied the rupture of single molecule junctions involving Au contacts and ODT. The experimental data of Huang et al. is included in Fig. 9b, where it is found that the calculated lifetimes closer resemble those from the experiment; specially taking into account that no fitting attempt was made seeking for agreement.

4.2 Results for contaminated metallic nanowires

Fig. 10 shows a scheme of the unit cell employed to simulate the pure (**Au-p**) and contaminated Au NWs considered here. The light weight elements taken into account as contaminants are a H atom (**Au-H**) and a C atom (**Au-C**). The grey circles represent Au atoms, which remain fixed at their positions during the relaxation processes. The latter consists in a local energy minimization procedure by means of the conjugate gradient method or a search of a MEP by means of the NEB method.

In the case of contaminated NWs the circle marked with an X represents the location the contaminant atom. This figure also shows the definition of the α_1, α_2 and α_3 bond angles, determined by the atoms relevant for the analysis of the rupture of the NW.
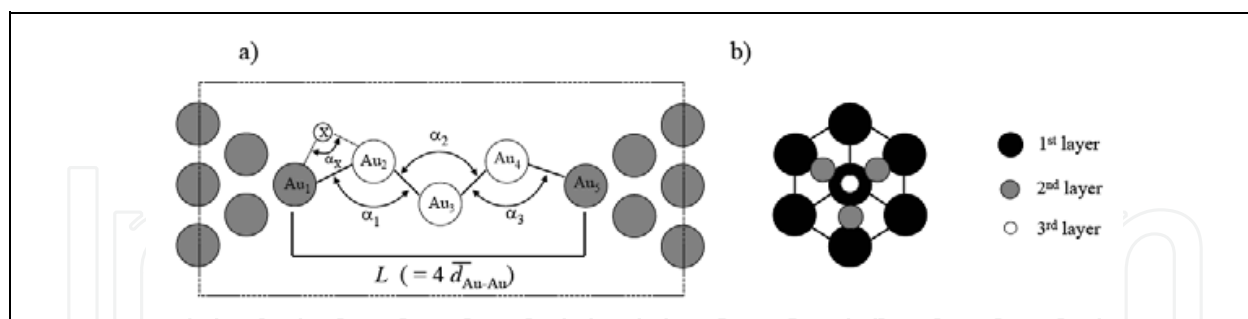

Fig. 10. Schematic representation of the unit cell employed in the present calculations: a) the rectangle indicates the extension of the unit cell. The grey circles represent the Au atoms fixed during the simulation. α_1, α_2 and α_3 are the bond angles between the Au atoms, and α_X is the angle defined by the atoms Au_1 – X – Au_2. *L* is the total chain length and $\bar{d}_{Au-Au}$ is the average Au – Au separation distance. b) Front view of the pyramid of Au atoms shown in a).

The length of the NW, *L*, is defined here as the distance between the atoms Au_1 and Au_5. We also define an average Au – Au separation, as $\bar{d}_{Au-Au} = L/4$. Fig. 10b shows the front view of one of the pyramid of Au atoms, represented as grey circles in Fig. 10a. The present systems

contains as a whole 18 atoms. It must be emphasized that in the case of calculations for pure Au NWs, the present systems deliver results that are close to those presented in the previous section for only four atoms in the unit cell. This indicates that the mechanical properties of the NW appear to be quite local, with a rather slight dependence from the bulky atomic environment.

The atomic impurity was located between the atoms Au_1 and Au_2. This choice was made because in the literature we found first principles calculations, similar to those performed here, where the H and C were positioned at a similar place, as well as between the Au_2 and Au_3 atoms, with similar results (Novaes et al., 2003; Skorodumova et al., 2007). As it will be found below, the present results agree with those where the impurity was located at another sites of the chain.

Structure and energetics of pure and contaminated Au NWs. For all the systems we shall refer to the *equilibrium* state as that where the derivative of the energy with respect to the elongation is equal to zero (ie. the external force, or stress, acting on the system is null). The rupture force will be considered to be the value of the force F_z where it presents a maximum at long elongations, being the force defined in Eq. 8 (da Silva et al., 2004; Jelínek et al., 2008; Novaes et al., 2003; Novaes et al., 2006; Rubio-Bollinger et al., 2001; Vélez et al., 2005; Vélez et al., 2008). Accordingly, we refer in the following to the "*at rupture*" state as that where the coordinates of the atoms are such that $\partial F_z / \partial \Delta z = 0$ (maximum force). With this definition, we are trying to address the status of the system just at the point where the NW is breaking by further force application. The structural information at the *equilibrium* and "*at rupture*" states of the NWs is summarized in Table 1 for the three systems types considered.

Considering the length difference between the "*at rupture*" and *equilibrium* states of the different systems, it is found that the stretching lengths of the **Au-p** and **Au-C** systems are 1.9 Å and 1.6 Å respectively, while the elongation of the **Au-H** system is considerably larger (2.6 Å). This fact bears direct consequences for the force constant k_z, as will be seen later on. Inspecting Table 1 it becomes clear that the equilibrium geometries of the contaminated

	Equilibrium geometries			„*At rupture*" geometries		
	Au-p	**Au-H**	**Au-C**	**Au-p**	**Au-H**	**Au-C**
L_e or L^* / Å	9.80	9.60	10.8	11.7	12.2	12.4
d (1,2) / Å	2.63	**2.76**	**3.78**	2.85	**3.58**	**3.87**
d (2,3) / Å	2.64	2.62	2.59	2.95	2.75	2.67
d (3,4) / Å	2.63	2.67	2.66	3.05	3.16	3.15
d (4,5) / Å	2.63	2.61	2.62	2.85	2.71	2.71
α_1 / °	139.5	149.6	161.8	179.3	178.6	178.5
α_2 / °	125.2	108.6	116.5	179.7	177.0	176.5
α_3 / °	139.7	157.4	136.0	179.9	178.5	178.2
α_X / °	---	**102.5**	**168.5**	---	**179.2**	**179.5**

Table 1. Structural information of the pure Au (**Au-p**) and hydrogen (**Au-H**) or carbon contaminated (**Au-C**) NWs at the equilibrium and close to rupture situations. In the first row, L_e is the equilibrium length of the NW, whereas L^* corresponds to length just before breakage occurs. Refer to Fig. 11 for an illustration of each of the geometries analyzed. The d (1,2) bond distance and the α_X bond angle of the impurity are in boldface.
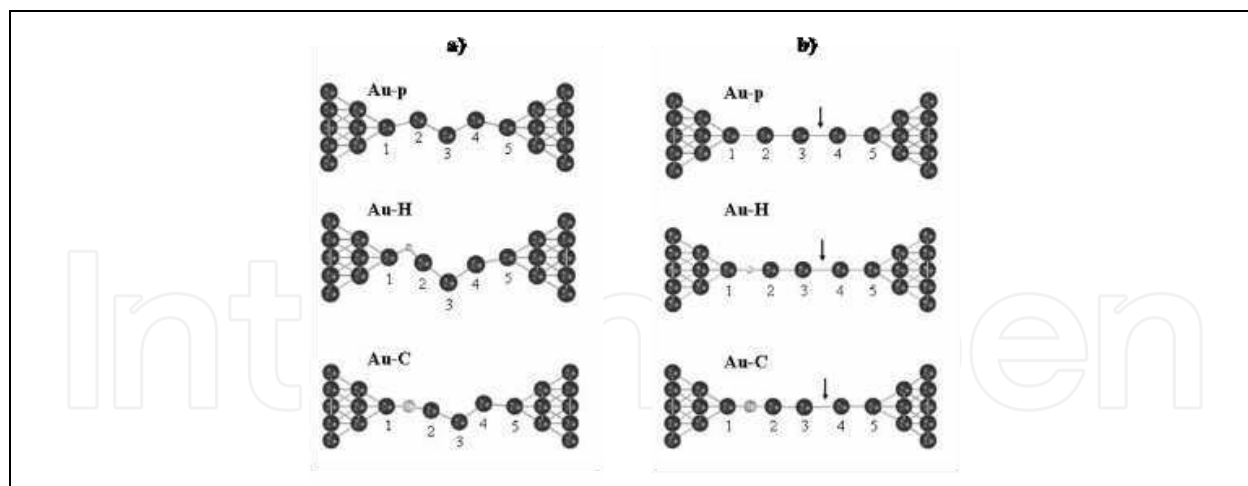
Fig. 11. a) Equilibrium geometries for the pure gold NW (**Au-p**) and contaminated with H (**Au-H**) and C (**Au-C**). b) Geometries just before rupture for stretched NWs. The arrows indicate the bond at which the NW breaks.

systems are very different from each other. Close to equilibrium, the presence of the H atom changes only slightly the d (1,2) bond distance, while the carbon atom inserts itself almost completely in the middle of this bond. This fact can be appreciated in the characteristics of the equilibrium configuration (see α_X bond angle and d (1,2) bond distance).

At the situation of the rupture, all three systems present a linear configuration and the distance of the Au_3 – Au_4 bond where it occurs is very similar (~3.1 Å). The contaminated systems arrive to the point of rupture with large Au – Au distances at the Au_1 – Au_2 bond; 3.58 Å for the **Au-H** system and 3.87 Å for the **Au-C** system. These figures indicate that our results are in a very good agreement with the Au – Au separation distances found experimentally (Kizuka, 2008; Kondo & Takayanagi, 2000; Legoas et al., 2002; Ohnishi et al., 1998; Rodrigues et al., 2000; Yanson et al., 1998) and with the first-principles calculations from other research groups (Novaes et al., 2003; Skorodumova et al., 2007).

Up to now, we have only explored the possibility of the incorporation of a single atomic impurity. In relation to this, it must be recognized that the extremely large Au – Au distances of 4 – 5 Å (Legoas et al., 2002), as well as consecutive distances of 3.5 – 4 Å (Kondo & Takayanagi, 2000; Ohnishi et al., 1998; Rodrigues & Ugarte, 2001a; Rodrigues et al., 2000) cannot be reproduced by our calculations. To tackle this point, more impurities should be considered, and probably other molecular species as proposed by other groups that performed first-principles calculations (Bahn et al., 2002; Galvão et al., 2004; Legoas et al., 2002; Novaes et al., 2003; Skorodumova & Simak, 2003; Skorodumova & Simak, 2004). However, the present approach is not devoted to predict all the Au – Au distances observed, but to understand the effect that an atomic impurity produces on a monatomic Au NW from energetic, geometrical, electronic and kinetic viewpoints.

Analysis of the time-stability of pure and contaminated NWs. In the following the kinetic aspects of the rupture process for the **Au-p**, **Au-H** and **Au-C** systems are considered. Fig. 12a shows the energy curves for the *unbroken* (u), *broken* (b) and *activated* (#) states as a function of the elongation (Δz) for **Au-H**. For **Au-p** the respective curves are similar to those shown in Fig. 6 for the 4-atom gold nanowire. The results obtained for **Au-C** have qualitatively the same features as those obtained for **Au-p**.
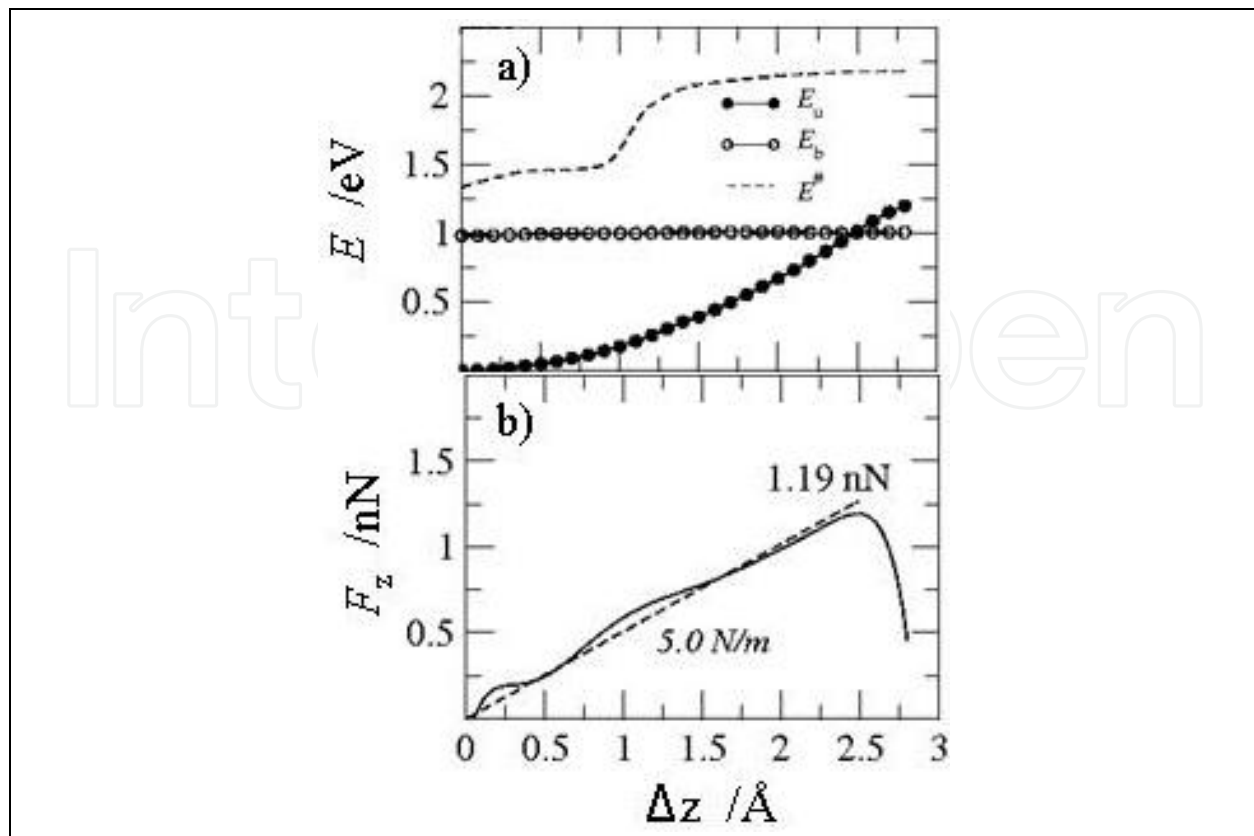
Fig. 12. a) Energy values corresponding to the *unbroken* state E_u, *broken* state E_b and activated state $E^\#$ of the system **Au-H** as a function of the elongation. b) Continuous curve: z component of the force acting on the system, F_z, calculated according to Eq. 8, as a function of Δz for **Au-H**. Broken line: Linear fit to F_z between zero and the maximum force. The maximum force F_z^{max} is indicated in normal typeset, while the force constant, k_z (slope of the broken lines), is denoted in italics.

In order to find candidate configurations for the *broken* (final in TST jargon) state at each elongation, molecular dynamics runs were performed at an elongation corresponding to the "*at-rupture*" configuration. This led to structures that looked like those illustrated for **Au-H** for the *broken* state configurations in Fig. 14 below.

We will perform a more detailed discussion of the reaction path for the rupture of the NWs below. We first consider the behaviour of the forces along the stretching procedure, since they are closely related to the energy curves of the *unbroken* state. In fact, the energy curves for the *unbroken* states in Fig. 12a may be used to calculate the longitudinal force F_z acting on this system according to Eq. 8. In Fig. 6, it was found that the stability limit of a monoatomic Au NW is reached at a force of 1.45 nN, which is close to the experimental value of 1.5 ± 0.3 nN (Kizuka, 2008; Rubio et al., 1996; Rubio-Bollinger et al., 2001). Fig. 12b shows F_z for the **Au-H** as a function of the elongation Δz. The maximum force F_z^{max} is also reported there. Table 2 compiles relevant information for this and the other systems under consideration in this study (**Au-p**, **Au-C**). For the **Au-p** system, the maximum force is 1.57 nN, also in agreement with the experiments and other theoretical values (da Silva et al., 2004; Rubio-Bollinger et al., 2001; Vélez et al., 2008). In the case of the contaminated systems, this value is somewhat lower (1.19 nN for **Au-H** and 1.14 nN for **Au-C**). First principles results from literature show the same trend (Novaes et al., 2003; Skorodumova et al., 2007).

	$F_z{}^{max}$, nN	k_z, N/m	$\Delta E^{\ddagger}(\Delta z)$, eV(Å)	
Au-p	1.57	9.1	0.99 (0.0)	0.22 (1.8)
Au-H	1.19	5.0	1.33 (0.0)	1.02 (2.7)
Au-C	1.14	8.2	1.12 (0.0)	1.10 (1.8)

Table 2. Maximum tensile force sustained before breakage ($F_z{}^{max}$, nN), force constant (k_z, N/m) and activation energy ($\Delta E^{\ddagger}$, eV) for the minimum energy path at the *equilibrium* and "*at-rupture*" geometries, for the systems **Au-p**, **Au-H** and **Au-C**. The activation energy for the rupture of the NW at each Δz is calculated as $\Delta E^{\ddagger} = E^{\#} - E_u$.

In their studies on the mechanic properties of monatomic Au NWs, (Rubio-Bollinger et al., 2001) found that these chains are five times harder than the massive electrodes. They evaluated from the experimental results the slopes of the force curves in the last stage of the elastic deformation, before the rupture of the NW, from a set of 200 experiments. The average value of the force constant for an average chain length was 8 N/m. The present calculations show that the behaviour of the force curves of the **Au-p**, **Au-H** and **Au-C** systems is quite elastic, as can be inferred from the linear fit of F_z between zero and the maximum force, shown in Fig. 12b for **Au-H** as a broken line. In the elastic deformation region, the force F_z may be written as:

$$F_z = k_z \, \Delta z \tag{9}$$

where k_z is the force constant of the system. The value of k_z found from the present calculations for **Au-p**, 9.1 N/m, is in perfect agreement with the experimental value reported in references (Rubio-Bollinger et al., 2001; Xu et al., 2003a). The contaminated systems present a remarkably different behaviour when compared between each other. The **Au-C** system has k_z =8.1 N/m, a very similar value to that of **Au-p**, but 1.6 larger than the value of this property for **Au-H** (k_z=5.0 N/m). These are interesting predictions, since up to date no measurements have been performed comparing pure and contaminated systems. A suitable fitting of the experimental data of this property could help to shed light on the type of impurity present when a NW exhibits large Au – Au separation distances.

Fig. 13 shows the energy of the system, E, as a function of the normalized reaction coordinate (NRC) for the system **Au-H** for some sample elongations. The corresponding configurations are presented in Fig. 14.

Fig. 13 shows that the **Au-H** system presents an energy curve along the minimum energy path that is more complex than those for **Au-p** and **Au-C** (not shown here). The distinctive feature for of **Au-H** is that at short elongations the energy curves present a minimum. This behavior is related to the incorporation of the hydrogen atom into the wire that takes place as the elongation proceeds. However, for the **Au-C** system, the C atom is incorporated into the wire since the beginning of the elongation. The minimum in the minimum energy path profile of the **Au-H** system disappears gradually with increasing elongation of the NW, remaining a shoulder at long elongations (see Fig. 13b).

The images of monatomic Au chains showing long separation distances (3.6 – 4 Å) were obtained by TEM and HRTEM using electron beam lithography for the fabrication of the NWs (Kizuka, 2008; Kondo & Takayanagi, 2000; Legoas et al., 2002; Ohnishi et al., 1998; Rodrigues & Ugarte, 2001a; Rodrigues et al., 2000). Under these experimental conditions, the elongation rate is not controlled and in principle not known. However, an estimation can be made looking at the pictures provided in some of these publications, as the one illustrated in
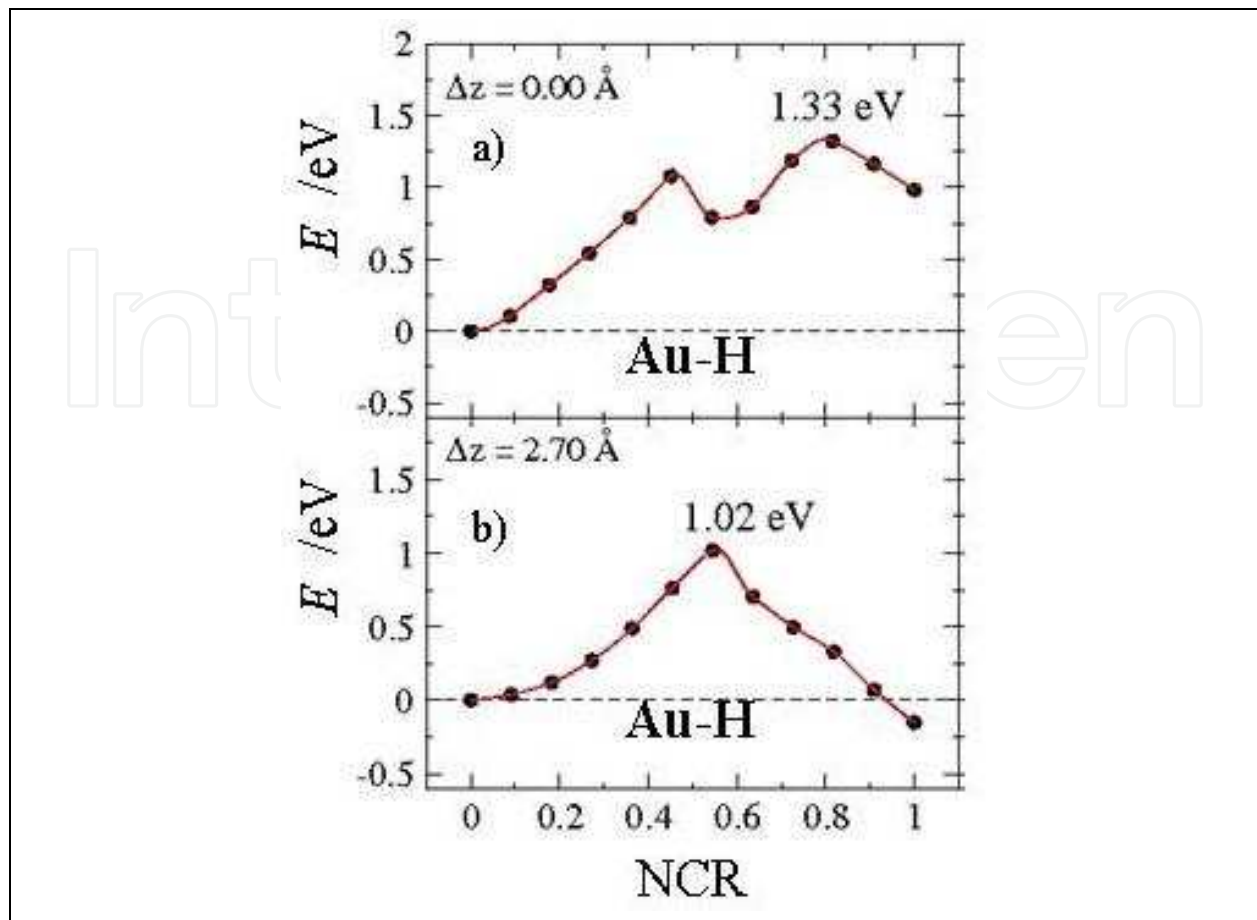
Fig. 13. System energy, *E*, as a function of the normalized reaction coordinate (NRC) along the reaction path between *unbroken* (u) and *broken* (b) states for different elongations Δ*z* of the NW. a), b) and c) correspond to the **Au-p** system, d), e) and f) to the **Au-H** system and g), h) and i) to the **Au-C** system. In all cases the energy of the system is referred to the energy of the *unbroken* state (u). The activation energies Δ*E*‡ and the corresponding elongations are given for each case.
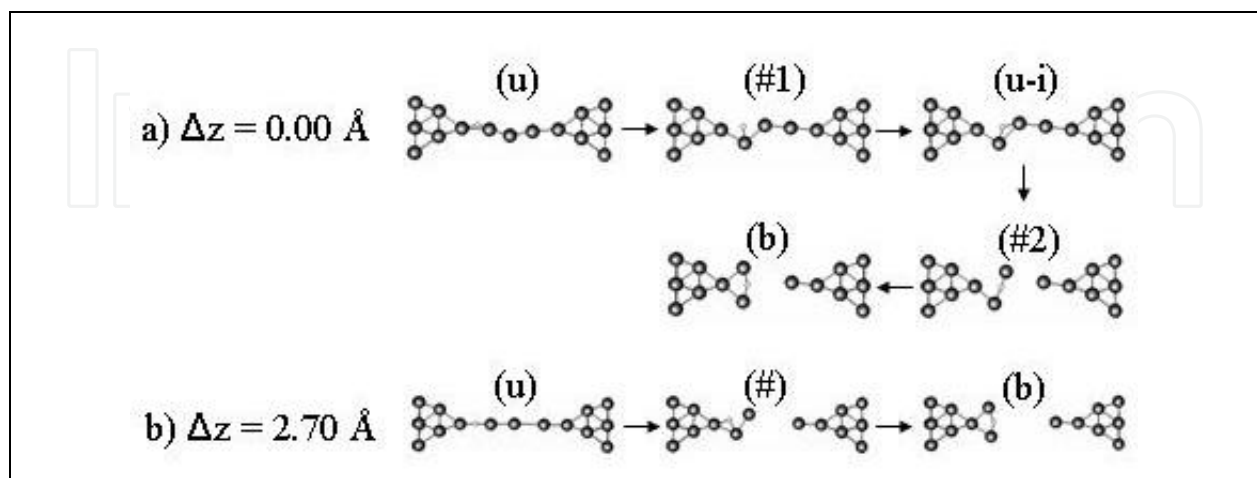

Fig. 14. Configurations of the *unbroken* (u), *activated* (#) and *broken* (b) states of the NW for each of the elongations Δ*z* whose energy curves along the reaction path are shown in Fig. 13 for **Au-H**.

Fig. 2 (Rodrigues & Ugarte, 2001a), and is found to be very slow, of the order of 0.1 nm/s in the final stage, allowing for a complete equilibration of the system at the atomic scale all along the elongation process. Thus, the rupture of the NWs in these experiments takes place in the timescale of a second, so that it can be inferred that the activation barriers must be quite high. In the static limit, the lifetime τ^* of a NW can be estimated from Eq 6. In this equation, we have used $\nu_u(\Delta z) = \nu_u = 3 \times 10^{12}$ Hz and T = 300 K. Similar values were used in references (Bürki et al., 2005; Rubio et al., 1996; Todorov et al., 2001; Vélez et al., 2008). Fig. 15 shows a plot of the decimal logarithm of the lifetime τ^* of the NW, as a function of the elongation force F_z for the **Au-p**, **Au-H** and **Au-C** systems.

It becomes evident from this figure that the contaminated NWs live considerably longer than Au-p NWs for all elongations. It is found that pure Au NW become unstable in the experimental time scale from an elongation which corresponds to d_{Au-Au} = 2.74 Å / atom on. In fact, for larger F_z (d_{Au-Au}), pure NWs should live less than 0.1 s. The remarkable behaviour of the **Au-H** system is due to the shape of the activation energy, discussed above in Fig. 13. Fig. 15 also supports the idea that impurities are responsible for the large Au – Au distances observed experimentally. These impurities, as stated above, modify geometrically the structure of the NWs, giving place to the occurrence of the anomalous large Au – Au distances. Furthermore, they modify the NW chemically by charge transfer and rearrangement, which in turn changes the potential energy surfaces so that for each elongation the contaminated NWs present higher activation barriers for the rupture than the pure NWs. Fig. 15 makes also plausible that stretched (contaminated) NWs may have lifetimes of the order of the second, sometimes even of the order of minutes (Ohnishi et al., 1998).
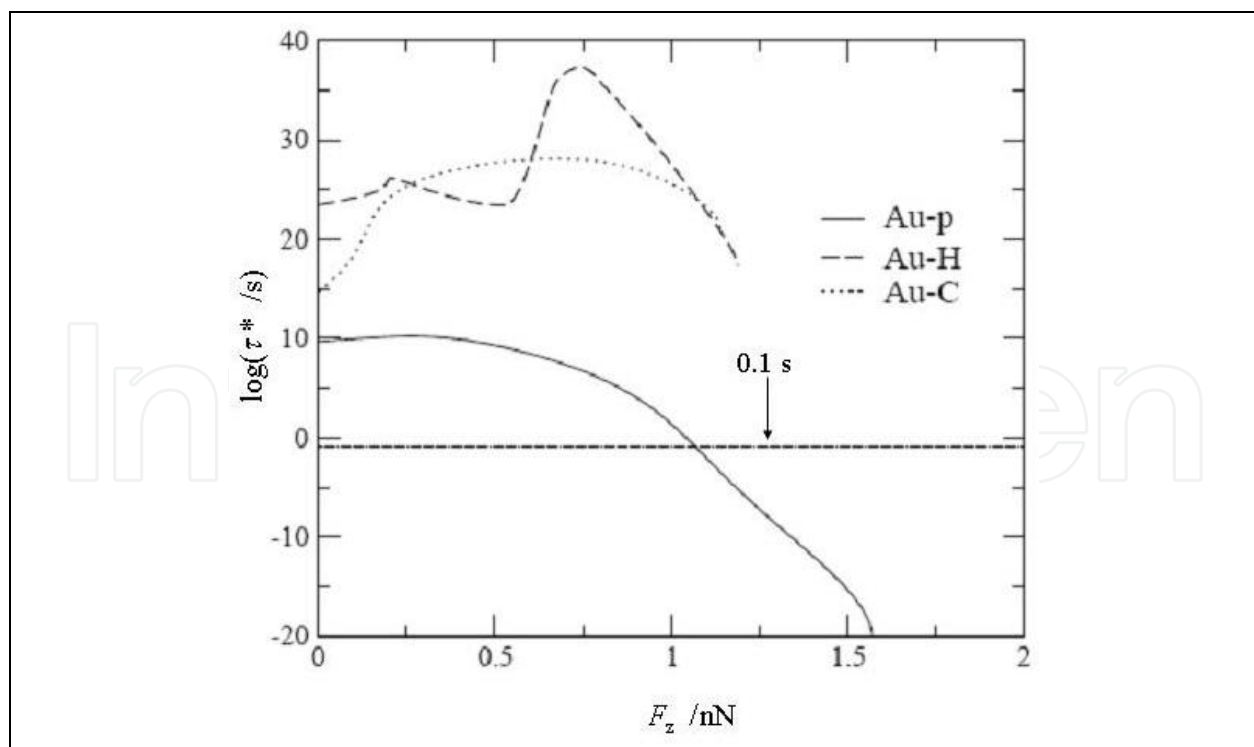

Fig. 15. Decimal logarithm of the lifetimes of the NWs corresponding to the systems **Au-p** (—), **Au-H** (---) and **Au-C** (• • • •) as a function of the elongation force F_z, calculated according to Eq. 6.

5. Long term stability of molecular nanowires. Effect of substituents on the Au – N nanojunction.

The formalism proposed in the previous sections could, in principle, be applied to study the mechanical and kinetic stability of single molecule nanowires. To the best of our knowledge, no such study has been yet attempted. One possible approximation to the long term stability problem is to estimate the kinetic barrier for the rupture of the nanowire by means of the *binding energy* of the system (E_b).

The mechanical properties of *ortho* substituted pyrazines bonded to planar gold clusters of 6 and 7 atoms have been studied using the same methodology described for the monatomic metallic nanowires. In Table 3, we summarize the values obtained for the binding energies (E_b) and rupture forces (F_{rup}) for the substituted pyrazines bonded to the 6-atom (Au_6) and the 7-atom (Au_{6+1}) gold clusters.

The systems studied are illustrated in Fig. 16. These systems are taken as a model for the last stage in the stretching of a Au – bipyridine nanojunction, and allow an assessment of the effect of a substituent in the molecule on the stability of the nanojunction.

The E_b values summarized in Table 3 were obtained as the energy difference between the minimum energy structure for each system and the final broken structure after stretching the nanojunction. In all cases the rupture occurred at the Au – N bond. F_{rup} values were obtained using Eq. 8.
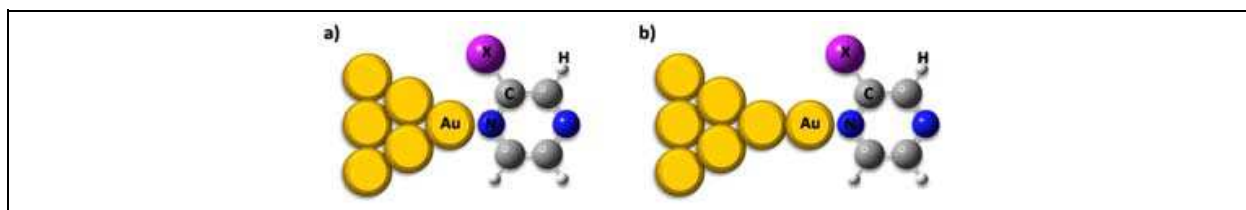

Fig. 16. Illustration of the models adopted to study the effect of ortho substituents on the mechanical stability of a Au – N nanojunction. a) Au_6 + X-pyrazine. b) Au_{6+1} + X-pyrizane.

X	σ	Au_6 + X-pyrazine		Au_{6+1} + X-pyrazine	
		E_b, eV	F_{rup}, nN	E_b, eV	F_{rup}, nN
NH$_2$	-0.66	0.795	1.16	0.913	1.26
CH$_3$	-0.17	0.731	1.07	0.828	1.13
H	0.00	0.671	1.00	0.778	1.09
Cl	0.23	0.596	0.82	0.689	0.98
CONH$_2$	0.36	0.549	0.77	---	---
CN	0.66	0.497	0.77	0.605	0.88
NO$_2$	0.78	0.409	0.48	0.560	0.73

Table 3. Hammett's σ (values taken from (Hansch et al., 1991)), binding energies (E_b) and rupture forces (F_{rup}) obtained from stretching experiments for Au_6 + X-pyrazines and Au_{6+1} X-pyrazines.

Using the E_b values as a *lower* limit for the activation energy to break the nanojunction, and using Eq. 6 with $\nu_u = 10^{12}$ Hz (a typical value for these systems as shown above), time constant values, τ^*, can be calculated for the different nanojunctions. The values for τ so obtained represent a *lower* limit for the lifetime of the nanojunctions. Interestingly, there is a

an excellent correlation between the logarithmic lifetime and a pure empirical parameter describing the electronic nature of the substituent such as Hammett's σ (Hansch et al., 1991), as illustrated in Fig. 17a.

Fig. 17b shows that a good correlation is also observed with respect to the calculated rupture force for the nanojunction. This is interesting since F_{rup} values can be obtained experimentally.

Note that the electronic properties of the substituent has a marked effect on the lifetime of the nanojunction, which ranges from 10^{-6} seconds for X = NO_2 to about 10^3 seconds for NH_2. On the other hand, only a slight effect of the substituent was found on the experimentally measured conductance of a structurally similar system (Venkataraman et al., 2007).

When the molecule binds to a less coordinated gold atom, such as in Au_{6+1} – X-pyrazine systems, the strength of the nanojunction increases, as reflected by the higher values obtained for both E_b and F_{rup}. This also causes an increase in the lifetime of the molecular junction, as illustrated in Fig. 17.
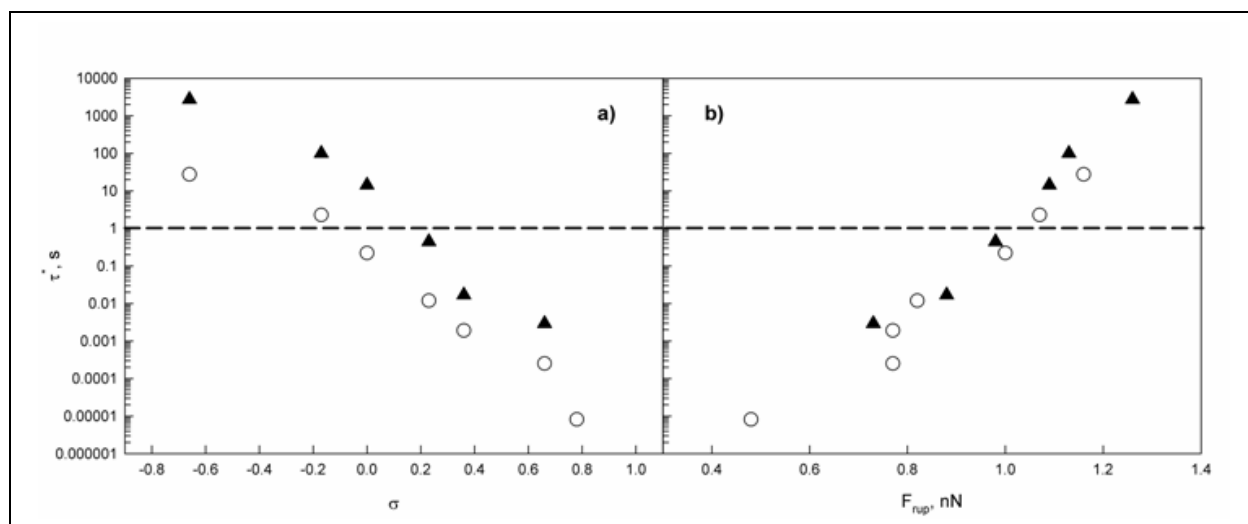

Fig. 17. Correlation between log τ, calculated as the lower limit for the nanojunction's lifetime and a) Hammett's σ and b) calculated rupture force (F_{rup}). In both plots, open circles represent the Au_6 + X-pyrazine systems, whereas filled triangles are for the Au_{6+1} – X-pyrazine systems.

6. Conclusions and perspectives

A comprehensive revision of the most recent advances with respect to the experimental techniques and computational simulations focused on the stability and mechanical properties of monatomic metallic and single molecule nanowires is presented.

We have established a simple model based on the *Transition State Theory* and using the *Minimum Energy Path* to study the long-term stability of nanowires in a time scale corresponding to that of the experimental observations. The utility of this model has been demonstrated for the quantitative evaluation of the effect of impurities in gold nanowires, as well as for a qualitative assessment of the effect exerted by a change in the electronic properties of a molecule in the temporal stability of a metal – molecule junction.

Some of the future work within this topic includes the analysis of other systems, including different metals and / or other chemical linkers for molecular nanowires. It would also be of

great interest to evaluate, if there is any, the correlation between the stability of the nanowire and its electronic properties, such as conductance.

7. References

Amorim, E. P. M.; da Silva, A. J. R. & da Silva, E. Z. (2008). Computer Simulations of Copper and Gold Nanowires and Single-wall Nanowires, *J. Phys. Chem. C*, Vol. 112, No.39, 15241-15246, ISSN: 1932-7447.

Amorim, E. P. M.; da Silva, A. J. R.; Fazzio, A. & da Silva, E. Z. (2007). Short linear atomic chains in copper nanowires, *Nanotechnology*, Vol. 18, No.14, 145701, ISSN: 0957-4484.

Anglada, E.; Torres, J. A.; Yndurain, F. & Soler, J. M. (2007). Formation of Gold Nanowires with Impurities: A First-Principles Molecular Dynamics Simulation, *Phys. Rev. Lett.*, Vol. 98, No.9, 096102-096104, ISSN: 0031-9007.

Auletta, T.; de Jong, M. R.; Mulder, A.; van Veggel, F. C. J. M.; Huskens, J.; Reinhoudt, D. N.; Zou, S.; Zapotoczny, S.; Schönherr, H.; Vancso, G. J. & Kuipers, L. (2004). β-Cyclodextrin Host–Guest Complexes Probed under Thermodynamic Equilibrium: Thermodynamics and AFM Force Spectroscopy, *J. Am. Chem. Soc.*, Vol. 126, No.5, 1577-1584, ISSN: 0002-7863.

Bahn, S. R.; Lopez, N.; Nørskov, J. K. & Jacobsen, K. W. (2002). Adsorption-induced restructuring of gold nanochains, *Phys. Rev. B*, Vol. 66, No.8, 081405 (pp 1-4), ISSN: 1098-0121.

Bahn, S. R. & Jacobsen, K. W. (2001). Chain Formation of Metal Atoms, *Phys. Rev. Lett.*, Vol. 87, No.26, 266101-1-266101-4, ISSN: 0031-9007.

Baskes, M. I.; Nelson, J. S. & Wright, A. F. (1989). Semiempirical modified embedded-atom potentials for silicon and germanium, *Phys. Rev. B*, Vol. 40, No.9, 6085-6100, ISSN: 1098-0121.

Batista, R. J. C.; Ordejon, P.; Chacham, H. & Artacho, E. (2007). Resistive and rectifying effects of pulling gold atoms at thiol-gold nanocontacts, *Phys. Rev. B*, Vol. 75, No.4, 041402-041404, ISSN: 1098-0121.

Beebe, J. M.; Engelkes, V. B.; Miller, L. L. & Frisbie, C. D. (2002). Contact Resistance in Metal-Molecule-Metal Junctions Based on Aliphatic SAMs: Effects of Surface Linker and Metal Work Function, *J. Am. Chem. Soc.*, Vol. 124, No.38, 11268-11269, ISSN: 0002-7863.

Bettini, J.; Sato, F.; Coura, P. Z.; Dantas, S. O.; Galvão, D. S. & Ugarte, D. (2006). Experimental realization of suspended atomic chains composed of different atomic species, *Nat Nano*, Vol. 1, No.3, 182-185, ISSN: 1748-3387.

Bonacic-Koutecky, V.; Burda, J.; Mitric, R.; Ge, M.; Zampella, G. & Fantucci, P. (2002). Density functional study of structural and electronic properties of bimetallic silver--gold clusters: Comparison with pure gold and silver clusters, *J. Chem. Phys.*, Vol. 117, No.7, 3120-3131, ISSN: 0021-9606.

Bürki, J.; Stafford, C. A. & Stein, D. L. (2005). Theory of Metastability in Simple Metal Nanowires, *Phys. Rev. Lett.*, Vol. 95, No.9, 090601, ISSN: 0031-9007.

Chen, F.; Li, X.; Hihath, J.; Huang, Z. & Tao, N. (2006). Effect of Anchoring Groups on Single-Molecule Conductance: Comparative Study of Thiol-, Amine-, and

Carboxylic-Acid-Terminated Molecules, *J. Am. Chem. Soc.*, Vol. 128, No.49, 15874-15881, ISSN: 0002-7863.

Cui, X. D.; Primak, A.; Zarate, X.; Tomfohr, J.; Sankey, O. F.; Moore, A. L.; Moore, T. A.; Gust, D.; Harris, G. & Lindsay, S. M. (2001). Reproducible Measurement of Single-Molecule Conductivity, *Science*, Vol. 294, No.5542, 571-574, ISSN: 0036-8075.

da Silva, E. Z.; da Silva, A. J. R. & Fazzio, A. (2001). How Do Gold Nanowires Break?, *Phys. Rev. Lett.*, Vol. 87, No.25, 256102, ISSN: 0031-9007.

da Silva, E. Z.; Novaes, F. D.; da Silva, A. J. R. & Fazzio, A. (2004). Theoretical study of the formation, evolution, and breaking of gold nanowires, *Phys. Rev. B*, Vol. 69, No.11, 115411 (pp 1-11), ISSN: 1098-0121.

De Maria, L. & Springborg, M. (2000). Electronic structure and dimerization of a single monatomic gold wire, *Chemical Physics Letters*, Vol. 323, No.3-4, 293-299, ISSN: 0009-2614.

Dreher, M.; Pauly, F.; Heurich, J.; Cuevas, J. C.; Scheer, E. & Nielaba, P. (2005). Structure and conductance histogram of atomic-sized Au contacts, *Phys. Rev. B*, Vol. 72, No.7, 075435-11, ISSN: 1098-0121.

Evans, E. & Ritchie, K. (1997). Dynamic strength of molecular adhesion bonds, *Biophysical Journal*, Vol. 72, No.4, 1541-1555, ISSN: 0006-3495.

Evans, E. (1999). Introductory Lecture Energy landscapes of biomolecular adhesion and receptor anchoring at interfaces explored with dynamic force spectroscopy, *Faraday Discussions*, Vol. 111, 1-16, ISSN: 1364-5498.

Evans, E. (2001). Probing the Relation Between Force-Lifetime and Chemistry in Single Molecular Bonds, *Annual Review of Biophysics and Biomolecular Structure*, Vol. 30, No.1, 105-128, ISSN: 1056-8700.

Eyring, H. (1935). The Activated Complex in Chemical Reactions, *J. Chem. Phys.*, Vol. 3, No.2, 107-115, ISSN: 0021-9606.

Galvão, D. S.; Rodrigues, V.; Ugarte, D. & Legoas, S. B. (2004). The role of carbon contamination in metallic nanowires, *Materials Research*, Vol. 7, 339-342, ISSN: 1516-1439.

Haiss, W.; Martín, S.; Leary, E.; Zalinge, H. v.; Higgins, S. J.; Bouffier, L. & Nichols, R. J. (2009). Impact of Junction Formation Method and Surface Roughness on Single Molecule Conductance, *The Journal of Physical Chemistry C*, Vol. 113, No.14, 5823-5833, ISSN: 1932-7447.

Haiss, W.; Nichols, R. J.; van Zalinge, H.; Higgins, S. J.; Bethel, D. & Schiffrin, D. J. (2004). Measurement of single molecule conductivity using the spontaneous formation of molecular wires, *Phys. Chem. Chem. Phys.*, Vol. 6, 4330-4337, ISSN: 14639076.

Haiss, W.; Wang, C.; Grace, I.; Batsanov, A. S.; Schiffrin, D. J.; Higgins, S. J.; Bryce, M. R.; Lambert, C. J. & Nichols, R. J. (2006). Precision control of single-molecule electrical junctions, *Nature Materials*, Vol. 5, No.12, 995-1002, ISSN: 1476-1122.

Haiss, W.; Wang, C.; Jitchati, R.; Grace, I.; Martín, S.; Batsanov, A. S.; Higgins, S.; Bryce, M. R.; Lambert, C. J.; Jensen, P. S. & Nichols, R. J. (2008). Variable contact gap single-molecule conductance determination for a series of conjugated molecular bridges, *Journal of Physics: Condensed Matter*, Vol. 20, No.37, 374119 (9pp), ISSN: 0953-9984.

Häkkinen, H.; Barnett, R. N.; Scherbakov, A. G. & Landman, U. (2000). Nanowire Gold Chains: Formation Mechanisms and Conductance, *J. Phys. Chem. B*, Vol. 104, No.39, 9063-9066, ISSN: 1520-6106.

Hansch, C.; Leo, A. & Taft, R. W. (1991). A Survey of Hammett Substituent Constants and Resonance and Field Parameters, *Chem. Rev.*, Vol. 91, No.2, 165-195, ISSN: 0009-2665.

He, H. X.; Shu, C.; Li, C. Z. & Tao, N. J. (2002). Adsorbate effect on the mechanical stability of atomically thin metallic wires, *Journal of Electroanalytical Chemistry*, Vol. 522, No.1, 26-32, ISSN: 0022-0728.

Henkelman, G. & Jonsson, H. (2000). Improved tangent estimate in the nudged elastic band method for finding minimum energy paths and saddle points, *J. Chem. Phys.*, Vol. 113, No.22, 9978-9985, ISSN: 0021-9606.

Henkelman, G.; Uberuaga, B. P. & Jonsson, H. (2000). A climbing image nudged elastic band method for finding saddle points and minimum energy paths, *J. Chem. Phys.*, Vol. 113, No.22, 9901-9904, ISSN: 0021-9606.

Hobi, E.; da Silva, A. J. R.; Novaes, F. D.; da Silva, E. Z. & Fazzio, A. (2005). Comment on "Contaminants in Suspended Gold Chains: An Ab Initio Molecular Dynamics Study", *Phys. Rev. Lett.*, Vol. 95, No.16, 169601 (p 1), ISSN: 0031-9007.

Hobi, E. Jr.; Fazzio, A. & da Silva, A. J. R. (2008). Temperature and Quantum Effects in the Stability of Pure and Doped Gold Nanowires, *Phys. Rev. Lett.*, Vol. 100, No.5, 056104 (pp 1-4), ISSN: 0031-9007.

Hou, S.; Ning, J.; Shen, Z.; Zhao, X. & Xue, Z. (2006). Influences of the molecule-electrode interface structure on the conducting characteristics of the gold-4,4 bipyridine-gold molecular junction, *Chem. Phys.*, Vol. 327, No.1, 1-9, ISSN: 0301-0104.

Hou, S.; Zhang, J.; Li, R.; Ning, J.; Han, R.; Shen, Z.; Zhao, X.; Xue, Z. & Wu, Q. (2005). First-principles calculation of the conductance of a single 4,4 bipyridine molecule, *Nanotechnology*, Vol. 16, No.2, 239-244, ISSN: 0957-4484.

Huang, Z. F.; Chen, F.; Bennett, P. A. & Tao, N. J. (2007a). Single Molecule Junctions Formed via Au-Thiol Contact: Stability and Breakdown Mechanism, *J. Am. Chem. Soc.*, Vol. 129, No.43, 13225-13231, ISSN: 0002-7863.

Huang, Z. F.; Xu, B. Q.; Chen, Y. C.; Ventra, M. D. & Tao, N. J. (2006). Measurement of Current-Induced Local Heating in a Single Molecule Junction, *Nano Lett.*, Vol. 6, No.6, 1240-1244, ISSN: 1530-6984.

Huang, Z.; Chen, F.; D'agosta, R.; Bennett, P. A.; Di Ventra, M. & Tao, N. (2007b). Local ionic and electron heating in single-molecule junctions, *Nature Nanotechnology*, Vol. 2, No.11, 698-703, ISSN: 1748-3387.

Hybertsen, M. S.; Venkataraman, L.; Klare, J. E.; Whalley, A. C.; Steigerwald, M. L. & Nuckolls, C. (2008). Amine-linked single-molecule circuits: systematic trends across molecular families, *Journal of Physics: Condensed Matter*, Vol. 20, No.37, 374115, ISSN: 0953-8984.

Jelínek, P.; Pérez, R.; Ortega, J. & Flores, F. (2008). Ab initio study of evolution of mechanical and transport properties of clean and contaminated Au nanowires along the deformation path, *Phys. Rev. B*, Vol. 77, No.11, 115447 (pp 1-12), ISSN: 1098-0121.

Kamenetska, M.; Koentopp, M.; Whalley, A. C.; Park, Y. S.; Steigerwald, M. L.; Nuckolls, C.; Hybertsen, M. S. & Venkataraman, L. (2009). Formation and Evolution of Single-Molecule Junctions, *Phys. Rev. Lett.*, Vol. 102, No.12, 126803-126804, ISSN: 0031-9007.

Ke, L.; Kotani, T.; van Schilfgaarde, M. & Bennett, P. A. (2007). Breakdown of a gold nanowire between electrodes, *Nanotechnology*, Vol. 18, No.42, 424002, ISSN: 0957-4484.

Kiguchi, M.; Miura, S.; Hara, K.; Sawamura, M. & Murakoshi, K. (2006). Conductance of a single molecule anchored by an isocyanide substituent to gold electrodes, *Appl. Phys. Lett.*, Vol. 89, No.21, 213104-3, ISSN: 0003-6951.

Kiguchi, M.; Miura, S.; Hara, K.; Sawamura, M. & Murakoshi, K. (2007). Conductance of single 1,4-disubstituted benzene molecules anchored to Pt electrodes, *Appl. Phys. Lett.*, Vol. 91, No.5, 053110-053113, ISSN: 0003-6951.

Kiguchi, M.; Miura, S.; Takahashi, T.; Hara, K.; Sawamura, M. & Murakoshi, K. (2008). Conductance of Single 1,4-Benzenediamine Molecule Bridging between Au and Pt Electrodes, *J. Phys. Chem. C*, Vol. 112, No.35, 13349-13352, ISSN: 1932-7447.

Kiguchi, M. & Murakoshi, K. (2006). Fabrication of stable Pd nanowire assisted by hydrogen in solution, *Appl. Phys. Lett.*, Vol. 88, No.25, 253112-253113, ISSN: 0003-6951.

Kim, B. S.; Beebe, J. M.; Jun, Y.; Zhu, X. Y. & Frisbie, C. D. (2006a). Correlation between HOMO Alignment and Contact Resistance in Molecular Junctions: Aromatic Thiols versus Aromatic Isocyanides, *J. Am. Chem. Soc.*, Vol. 128, No.15, 4970-4971, ISSN: 0002-7863.

Kim, Y. H.; Tahir-Kheli, J.; Schultz, P. A.; Goddard, W. A. & III (2006b). First-principles approach to the charge-transport characteristics of monolayer molecular-electronics devices: Application to hexanedithiolate devices, *Phys. Rev. B*, Vol. 73, No.23, 235419-10, ISSN: 1098-0121.

Kizuka, T. (2008). Atomic configuration and mechanical and electrical properties of stable gold wires of single-atom width, *Phys. Rev. B*, Vol. 77, No.15, 155401 (pp 1-11), ISSN: 1098-0121.

Koizumi, H.; Oshima, Y.; Kondo, Y. & Takayanagi, K. (2001). Quantitative high-resolution microscopy on a suspended chain of gold atoms, *Ultramicroscopy*, Vol. 88, No.1, 17-24, ISSN: 0304-3991.

Kondo, Y. & Takayanagi, K. (1997). Gold Nanobridge Stabilized by Surface Structure, *Phys. Rev. Lett.*, Vol. 79, No.18, 3455, ISSN: 0031-9007.

Kondo, Y. & Takayanagi, K. (2000). Synthesis and Characterization of Helical Multi-Shell Gold Nanowires, *Science*, Vol. 289, No.5479, 606-608, ISSN: 0036-8075.

Krüger, D.; Fuchs, H.; Rousseau, R.; Marx, D. & Parrinello, M. (2002). Pulling Monatomic Gold Wires with Single Molecules: An Ab Initio Simulation, *Phys. Rev. Lett.*, Vol. 89, No.18, 186402, ISSN: 0031-9007.

Krüger, D.; Rousseau, R.; Fuchs, H. & Marx, D. (2003). Towards "Mechanochemistry": Mechanically Induced Isomerizations of Thiolate-Gold Clusters, *Angew. Chem. Int. Ed. Eng.*, Vol. 42, No.20, 2251-2253, ISSN: 1433-7851.

Legoas, S. B.; Galvao, D. S.; Rodrigues, V. & Ugarte, D. (2002). Origin of Anomalously Long Interatomic Distances in Suspended Gold Chains, *Phys. Rev. Lett.*, Vol. 88, No.7, 076105 (pp 1-4), ISSN: 0031-9007.

Legoas, S. B.; Rodrigues, V.; Ugarte, D. & Galvão, D. S. (2004). Contaminants in Suspended Gold Chains: An Ab Initio Molecular Dynamics Study, *Phys. Rev. Lett.*, Vol. 93, No.21, 216103 (pp 1-4), ISSN: 0031-9007.

Li et al, C. Z. (1999). Fabrication of stable metallic nanowires with quantized conductance, *Nanotechnology*, Vol. 10, No.2, 221, ISSN: 0957-4484.

Li, C. Z. & Tao, N. J. (1998). Quantum transport in metallic nanowires fabricated by electrochemical deposition/dissolution, *Appl. Phys. Lett.*, Vol. 72, No.8, 894-896, ISSN: 0003-6951.

Li, C.; Pobelov, I.; Wandlowski, T.; Bagrets, A.; Arnold, A. & Evers, F. (2007b). Charge Transport in Single Au | Alkanedithiol | Au Junctions: Coordination Geometries and Conformational Degrees of Freedom, *J. Am. Chem. Soc.*, Vol. 130, No.1, 318-326, ISSN: 0002-7863.

Li, C.; Pobelov, I.; Wandlowski, T.; Bagrets, A.; Arnold, A. & Evers, F. (2007a). Charge Transport in Single Au | Alkanedithiol | Au Junctions: Coordination Geometries and Conformational Degrees of Freedom, *J. Am. Chem. Soc.*, Vol. 130, No.1, 318-326, ISSN: 0002-7863.

Li, Q.; Wu, X.; Huang, J. & Yang, J. (2005). Electronic transport property of 4,4'-bipyridine molecular junction, *Ultramicroscopy*, Vol. 105, No.1-4, 293-298, ISSN: 0304-3991.

Li, X.; He, J.; Hihath, J.; Xu, B.; Lindsay, S. M. & Tao, N. (2006a). Conductance of Single Alkanedithiols: Conduction Mechanism and Effect of Molecule-Electrode Contacts, *J. Am. Chem. Soc.*, Vol. 128, No.6, 2135-2141, ISSN: 0002-7863.

Li, Z. L.; Zou, B.; Wang, C. K. & Luo, Y. (2006b). Effects of Electrode Distances on Geometric Structure and Electronic Transport Properties of Molecular 4,4'-Bipyridine Junction, *Journal of Physics: Conference Series*, Vol. 29, 110-114, ISSN: 1742-6596.

Li, Z. L.; Zou, B.; Wang, C. K. & Luo, Y. (2006c). Electronic transport properties of molecular bipyridine junctions: Effects of isomer and contact structures, *Phys. Rev. B*, Vol. 73, No.7, 075326-075327, ISSN: 1098-0121.

Lorenz, R.; Georg, H.; Mathis, G.; Jean-Luc, B. & Egbert, Z. (2006). Stretching and Breaking of a Molecular Junction, *Small*, Vol. 2, No.12, 1468-1475, ISSN: 1613-6829.

Martín, S.; Haiss, W.; Higgins, S.; Cea, P.; Lopez, M. C. & Nichols, R. J. (2008). A Comprehensive Study of the Single Molecule Conductance of α,ω-Dicarboxylic Acid-Terminated Alkanes, *J. Phys. Chem. C*, Vol. 112, No.10, 3941-3948, ISSN: 1932-7447.

Merkel, R.; Nassoy, P.; Leung, A.; Ritchie, K. & Evans, E. (1999). Energy landscapes of receptor-ligand bonds explored with dynamic force spectroscopy, *Nature*, Vol. 397, No.6714, 50-53, ISSN: 0028-0836.

Michael, L. M. & Michael, P. (2007). Computing Reaction Pathways on Molecular Potential Energy Surfaces, In: *Reviews in Computational Chemistry Vol. 4*, Kenny, B. L. (Ed.), 35-65,

Mills, G. & Jónsson, H. (1994). Quantum and thermal effects in H2 dissociative adsorption: Evaluation of free energy barriers in multidimensional quantum systems, *Phys. Rev. Lett.*, Vol. 72, No.7, 1124, ISSN: 0031-9007.

Nakamura, A.; Brandbyge, M.; Hansen, L. B. & Jacobsen, K. W. (1999). Density Functional Simulation of a Breaking Nanowire, *Phys. Rev. Lett.*, Vol. 82, No.7, 1538, ISSN: 0031-9007.

Nakamura, J.; Kobayashi, N. & Aono, M. (2001). Electronic states and structural stability of gold nanowires, *RIKEN Review*, Vol. 2001, No.37, 17-20, ISSN: 0919-3405.

Novaes, F. D.; da Silva, A. J. R.; da Silva, E. Z. & Fazzio, A. (2003). Effect of Impurities in the Large Au-Au Distances in Gold Nanowires, *Phys. Rev. Lett.*, Vol. 90, No.3, 036101 (pp 1-4), ISSN: 0031-9007.

Novaes, F. D.; da Silva, A. J. R.; da Silva, E. Z. & Fazzio, A. (2006). Oxygen Clamps in Gold Nanowires, *Phys. Rev. Lett.*, Vol. 96, No.1, 016104 (pp 1-4), ISSN: 0031-9007.

O'Hanlon, J. F. (2001). *A User's Guide to Vacuum Technology*, John Wiley & Sons, Inc, ISBN: 9780471270522, Hoboken, NJ.

Ohnishi, H.; Kondo, Y. & Takayanagi, K. (1998). Quantized conductance through individual rows of suspended gold atoms, *Nature*, Vol. 395, No.6704, 780-783, ISSN: 0028-0836.

Okamoto, M. & Takayanagi, K. (1999). Structure and conductance of a gold atomic chain, *Phys. Rev. B*, Vol. 60, No.11, 7808-7811, ISSN: 1098-0121.

Park, Y. S.; Whalley, A. C.; Kamenetska, M.; Steigerwald, M. L.; Hybertsen, M. S.; Nuckolls, C. & Venkataraman, L. (2007). Contact Chemistry and Single-Molecule Conductance: A Comparison of Phosphines, Methyl Sulfides, and Amines, *J. Am. Chem. Soc.*, Vol. 129, No.51, 15768-15769, ISSN: 0002-7863.

Park, Y. S.; Widawsky, J. R.; Kamenetska, M.; Steigerwald, M. L.; Hybertsen, M. S.; Nuckolls, C. & Venkataraman, L. (2009). Frustrated Rotations in Single-Molecule Junctions, *J. Am. Chem. Soc.*, Vol. 131, No.31, 10820-10821, ISSN: 0002-7863.

Patrone, L.; Palacin, S. & Bourgoin, J. P. (2003a). Direct comparison of the electronic coupling efficiency of sulfur and selenium alligator clips for molecules adsorbed onto gold electrodes, *Applied Surface Science*, Vol. 212-213, 446-451, ISSN: 0169-4332.

Patrone, L.; Palacin, S.; Charlier, J.; Armand, F.; Bourgoin, J. P.; Tang, H. & Gauthier, S. (2003b). Evidence of the Key Role of Metal-Molecule Bonding in Metal-Molecule-Metal Transport Experiments, *Phys. Rev. Lett.*, Vol. 91, No.9, 096802, ISSN: 0031-9007.

Paulsson, M.; Krag, C.; Frederiksen, T. & Brandbyge, M. (2008). Conductance of Alkanedithiol Single-Molecule Junctions: A Molecular Dynamics Study, *Nano Lett.*, Vol. 9, No.1, 117-121, ISSN: 1530-6984.

Perez-Jimenez, A. (2005). Uncovering Transport Properties of 4,4'-Bipyridine/Gold Molecular Nanobridges, *J. Phys. Chem. B*, Vol. 109, No.20, 10052-10060, ISSN: 1520-6106.

Pu, Q.; Leng, Y.; Tsetseris, L.; Park, H. S.; Pantelides, S. T. & Cummings, P. T. (2007a). Molecular dynamics simulations of stretched gold nanowires: The relative utility of different semiempirical potentials, *J. Chem. Phys.*, Vol. 126, No.14, 144707-6, ISSN: 0021-9606.

Pu, Q.; Leng, Y.; Zhao, X. & Cummings, P. T. (2007b). Molecular simulations of stretching gold nanowires in solvents, *Nanotechnology*, Vol. 18, No.42, 424007, ISSN: 0957-4484.

Quek, S. Y.; Venkataraman, L.; Choi, H. J.; Louie, S. G.; Hybertsen, M. S. & Neaton, J. B. (2007). Amine-Gold Linked Single-Molecule Circuits: Experiment and Theory, *Nano Lett.*, Vol. 7, No.11, 3477-3482, ISSN: 1530-6984.

Quek, S. Y.; Kamenetska, M.; Steigerwald, M. L.; Choi, H. J.; Louie, S. G.; Hybertsen, M. S.; Neaton, J. B. & Venkataraman, L. (2009). Mechanically controlled binary conductance switching of a single-molecule junction, *Nat Nano*, Vol. 4, No.4, 230-234, ISSN: 1748-3387.

Quinn, J. R.; Foss, F. W.; Venkataraman, L.; Hybertsen, M. S. & Breslow, R. (2007). Single-Molecule Junction Conductance through Diaminoacenes, *J. Am. Chem. Soc.*, Vol. 129, No.21, 6714-6715, ISSN: 0002-7863.

Rodrigues, V.; Bettini, J.; Rocha, A. R.; Rego, L. G. C. & Ugarte, D. (2002). Quantum conductance in silver nanowires: Correlation between atomic structure and transport properties, *Phys. Rev. B*, Vol. 65, No.15, 153402, ISSN: 1098-0121.

Rodrigues, V. & Ugarte, D. (2001a). Real-time imaging of atomistic process in one-atom-thick metal junctions, *Phys. Rev. B*, Vol. 63, No.7, 073405 (pp 1-4), ISSN: 1098-0121.

Rodrigues, V. & Ugarte, D. (2001b). Structural and electronic properties of gold nanowires, *Eur. Phys. J. D*, Vol. 16, No.1-3, 395-398, ISSN: 1434-6060.

Rodrigues, V. & Ugarte, D. (2002). Quantum conductance properties of metal nanowires, *Materials Science and Engineering B*, Vol. 96, No.2, 188-192, ISSN: 0921-5107.

Rodrigues, V.; Bettini, J.; Silva, P. C. & Ugarte, D. (2003). Evidence for Spontaneous Spin-Polarized Transport in Magnetic Nanowires, *Phys. Rev. Lett.*, Vol. 91, No.9, 096801, ISSN: 0031-9007.

Rodrigues, V.; Fuhrer, T. & Ugarte, D. (2000). Signature of Atomic Structure in the Quantum Conductance of Gold Nanowires, *Phys. Rev. Lett.*, Vol. 85, No.19, 4124-4127, ISSN: 0031-9007.

Rubio, G.; Agraït, N. & Vieira, S. (1996). Atomic-Sized Metallic Contacts: Mechanical Properties and Electronic Transport, *Phys. Rev. Lett.*, Vol. 76, No.13, 2302-2305, ISSN: 0031-9007.

Rubio-Bollinger, G.; Bahn, S. R.; Agraït, N.; Jacobsen, K. W. & Vieira, S. (2001). Mechanical Properties and Formation Mechanisms of a Wire of Single Gold Atoms, *Phys. Rev. Lett.*, Vol. 87, No.2, 026101 (pp 1-4), ISSN: 0031-9007.

Sánchez-Portal, D.; Artacho, E.; Junquera, J.; Ordejón, P.; García, A. & Soler, J. M. (1999). Stiff Monatomic Gold Wires with a Spinning Zigzag Geometry, *Phys. Rev. Lett.*, Vol. 83, No.19, 3884-3887, ISSN: 0031-9007.

Sato, F.; Moreira, A. S.; Bettini, J.; Coura, P. Z.; Dantas, S. O.; Ugarte, D. & Galvao, D. S. (2006a). On the Formation of Copper Linear Atomic Suspended Chains, *Condensed Matter*, arXiv:cond-mat/0602092v1.

Sato, F.; Moreira, A. S.; Bettini, J.; Coura, P. Z.; Dantas, S. O.; Ugarte, D. & Galvao, D. S. (2006b). Transmission electron microscopy and molecular dynamics study of the formation of suspended copper linear atomic chains, *Phys. Rev. B*, Vol. 74, No.19, 193401-193404, ISSN: 1098-0121.

Schönherr, H.; Beulen, M. W. J.; Bügler, J.; Huskens, J.; van Veggel, F. C. J. M.; Reinhoudt, D. N. & Vancso, G. J. (2000). Individual Supramolecular Host–Guest Interactions Studied by Dynamic Single Molecule Force Spectroscopy, *J. Am. Chem. Soc.*, Vol. 122, No.20, 4963-4967, ISSN: 0002-7863.

Skorodumova, N. V. & Simak, S. I. (2003). Stability of gold nanowires at large Au-Au separations, *Phys. Rev. B*, Vol. 67, No.12, 121404 (pp 1-4), ISSN: 1098-0121.

Skorodumova, N. V. & Simak, S. I. (2004). Stabilization of monoatomic gold wires by carbon impurities, *Solid State Communications*, Vol. 130, No.11, 755-757, ISSN: 0038-1098.

Skorodumova, N. V.; Simak, S. I.; Kochetov, A. E. & Johansson, B. (2007). Ab initio study of electronic and structural properties of gold nanowires with light-element impurities, *Phys. Rev. B*, Vol. 75, No.23, 235440 (pp 1-4), ISSN: 1098-0121.

Sørensen, M. R.; Brandbyge, M. & Jacobsen, K. W. (1998). Mechanical deformation of atomic-scale metallic contacts: Structure and mechanisms, *Phys. Rev. B*, Vol. 57, No.6, 3283, ISSN: 1098-0121.

Sørensen, M. R.; Jacobsen, K. W. & Jónsson, H. (1996). Thermal Diffusion Processes in Metal-Tip-Surface Interactions: Contact Formation and Adatom Mobility, *Phys. Rev. Lett.*, Vol. 77, No.25, 5067, ISSN: 0031-9007.

Stadler, R.; Thygesen, K. S. & Jacobsen, K. W. (2005). Forces and conductances in a single-molecule bipyridine junction, *Phys. Rev. B*, Vol. 72, No.24, 241401-241404, ISSN: 1098-0121.

Stolberg, L.; Lipkowski, J. & Irish, D. E. (1990). Adsorption of pyridine at the Au(110) - solution interface, *Journal of Electroanalytical Chemistry*, Vol. 296, No.1, 171-189, ISSN: 0022-0728.

Takai, Y.; Kawasaki, T.; Kimura, Y.; Ikuta, T. & Shimizu, R. (2001). Dynamic Observation of an Atom-Sized Gold Wire by Phase Electron Microscopy, *Phys. Rev. Lett.*, Vol. 87, No.10, 106105, ISSN: 0031-9007.

Todorov, T. N.; Hoekstra, J. & Sutton, A. P. (2001). Current-Induced Embrittlement of Atomic Wires, *Phys. Rev. Lett.*, Vol. 86, No.16, 3606, ISSN: 0031-9007.

Torres, J. A.; Tosatti, E.; Dal Corso, A.; Ercolessi, F.; Kohanoff, J. J.; Di Tolla, F. D. & Soler, J. M. (1999). The puzzling stability of monatomic gold wires, *Surface Science*, Vol. 426, No.3, L441-L446, ISSN: 0039-6028.

Ulrich, J.; Esrail, D.; Pontius, W.; Venkataraman, L.; Millar, D. & Doerrer, L. H. (2006). Variability of Conductance in Molecular Junctions, *J. Phys. Chem. B*, Vol. 110, No.6, 2462-2466, ISSN: 1520-6106.

van Ruitenbeek, J.; Scheer, E. & Weber, H. (2005). Contacting Individual Molecules Using Mechanically Controllable Break Junctions, In: *Introducing Molecular Electronics*, Cuniberti, G., Fagas, G., and Richter, K. (Ed.), 253-274, Springer Berlin Heidelberg, ISBN: 1616-6361.

Vélez, P.; Dassie, S. A. & Leiva, E. P. M. (2005). First Principles Calculations of Mechanical Properties of 4,4'-Bipyridine Attached to Au Nanowires, *Phys. Rev. Lett.*, Vol. 95, No.4, 045503-045504, ISSN: 0031-9007.

Vélez, P.; Dassie, S. A. & Leiva, E. P. M. (2008). When do nanowires break? A model for the theoretical study of the long-term stability of monoatomic nanowires, *Chem. Phys. Lett.*, Vol. 460, No.1-3, 261-265, ISSN: 0009-2614.

Vélez, P.; Dassie, S. A. & Leiva, E. P. M. (2007). Understanding the properties of nanocontacts. Recent advances in experiment and theory, In: *Recent Advances in Nanoscience*, Mariscal, M. M. and Dassie, S. A. (Ed.), 1-38, Research Signpost, ISBN: 978-81-308-0207-7, Kerala, India.

Venkataraman, L.; Klare, J. E.; Tam, I. W.; Nuckolls, C.; Hybertsen, M. S. & Steigerwald, M. L. (2006a). Single-Molecule Circuits with Well-Defined Molecular Conductance, *Nano Lett.*, Vol. 6, No.3, 458-462, ISSN: 1530-6984.

Venkataraman, L.; Park, Y. S.; Whalley, A. C.; Nuckolls, C.; Hybertsen, M. S. & Steigerwald, M. L. (2007). Electronics and Chemistry: Varying Single-Molecule Junction Conductance Using Chemical Substituents, *Nano Lett.*, Vol. 7, No.2, 502-506, ISSN: 1530-6984.

Venkataraman, L.; Klare, J. E.; Nuckolls, C.; Hybertsen, M. S. & Steigerwald, M. L. (2006b). Dependence of single-molecule junction conductance on molecular conformation, *Nature*, Vol. 442, No.7105, 904-907, ISSN: 0028-0836.

Villarba, M. & Jónsson, H. (1994). Diffusion mechanisms relevant to metal crystal growth: Pt/Pt(111), *Surface Science*, Vol. 317, No.1-2, 15-36, ISSN: 0039-6028.

Vineyard, G. H. (1957). Frequency factors and isotope effects in solid state rate processes, *Journal of Physics and Chemistry of Solids*, Vol. 3, No.1-2, 121-127, ISSN: 0022-3697.

Wu, X.; Li, Q.; Huang, J. & Yang, J. (2005). Nonequilibrium electronic transport of 4,4'-bipyridine molecular junction, *J. Chem. Phys.*, Vol. 123, No.18, 184712-184716, ISSN:

Xu, B.; Xiao, X. & Tao, N. J. (2003a). Measurements of Single-Molecule Electromechanical Properties, *J. Am. Chem. Soc.*, Vol. 125, No.52, 16164-16165, ISSN: 0002-7863.

Xu, B. Q.; Li, X. L.; Xiao, X. Y.; Sakaguchi, H. & Tao, N. J. (2005). Electromechanical and Conductance Switching Properties of Single Oligothiophene Molecules, *Nano Lett.*, Vol. 5, No.7, 1491-1495, ISSN: 1530-6984.

Xu, B.; He, H.; Boussaad, S. & Tao, N. J. (2003b). Electrochemical properties of atomic-scale metal wires, *Electrochimica Acta*, Vol. 48, No.20-22, 3085-3091, ISSN: 0013-4686.

Xu, B. & Tao, N. J. (2003). Measurement of Single-Molecule Resistance by Repeated Formation of Molecular Junctions, *Science*, Vol. 301, No.5637, 1221-1223, ISSN: 0021-9606.

Yanson, A. I.; Bollinger, G. R.; van den Brom, H. E.; Agraït, N. & van Ruitenbeek, J. M. (1998). Formation and manipulation of a metallic wire of single gold atoms, *Nature*, Vol. 395, No.6704, 783-785, ISSN: 0028-0836.

Yasuda, S.; Yoshida, S.; Sasaki, J.; Okutsu, Y.; Nakamura, T.; Taninaka, A.; Takeuchi, O. & Shigekawa, H. (2006). Bond Fluctuation of S/Se Anchoring Observed in Single-Molecule Conductance Measurements using the Point Contact Method with Scanning Tunneling Microscopy, *J. Am. Chem. Soc.*, Vol. 128, No.24, 7746-7747, ISSN: 0002-7863.

Yoshida, M.; Kurui, Y.; Oshima, Y. & Takayanagi, K. (2007). In situ Observation of the Electrical Conductance of the Bridged Single Fullerene using TEM-STM, *Microscopy and Microanalysis*, Vol. 13, No.Supplement S02, 748-749, ISSN: 1431-9276.

Zhang, C.; Barnett, R. N. & Landman, U. (2008). Bonding, Conductance, and Magnetization of Oxygenated Au Nanowires, *Phys. Rev. Lett.*, Vol. 100, No.4, 046801-046804, ISSN: 0031-9007.

Zoloff Michoff, M. E.; Vélez, P. & Leiva, E. P. M. (2009). Substituent Effect on the Mechanical Properties of Au–N Nanojunctions, *J. Phys. Chem. C*, Vol. 113, No.9, 3850-3854, ISSN: 1932-7447.

Zou, S.; Schonherr, H. & Vancso, G. J. (2005). Force Spectroscopy of Quadruple H-Bonded Dimers by AFM: Dynamic Bond Rupture and Molecular Time–Temperature Superposition, *J. Am. Chem. Soc.*, Vol. 127, No.32, 11230-11231, ISSN: 0002-7863.

Electrodeposited Nanowires and their Applications

Edited by Nicoleta Lupu

The book offers a new and complex perspective on the fabrication and use of electrodeposited nanowires for the design of efficient and competitive applications. While not pretending to be comprehensive, the book is addressing not only to researchers specialized in this field, but also to Ph.D. students, postdocs and experienced technical professionals.

How to reference

In order to correctly reference this scholarly work, feel free to copy and paste the following:

Martin E. Zoloff Michoff, Patricio Vélez, Sergio A. Dassie and Ezequiel P. M. Leiva (2010). Computational Tools to Study and Predict the Long-Term Stability of Nanowires., Electrodeposited Nanowires and their Applications, Nicoleta Lupu (Ed.), ISBN: 978-953-7619-88-6, InTech, Available from:
http://www.intechopen.com/books/electrodeposited-nanowires-and-their-applications/computational-tools-to-study-and-predict-the-long-term-stability-of-nanowires-

INTECH

open science | open minds